Pure Lagrangian and semi-Lagrangian finite element methods for the numerical solution of Navier-Stokes equations

M. Benítez[a], A. Bermúdez[b]

[a] *Departamento de Matemáticas, Universidade da Coruña, c/ Mendizábal s/n, 15403 Ferrol, Spain*
[b] *Departamento de Matemática Aplicada, Universidade de Santiago de Compostela, c/ Lope Gómez de Marzoa s/n, 15786 Santiago de Compostela, Spain*

Abstract

In this paper we propose a unified formulation to introduce Lagrangian and semi-Lagrangian velocity and displacement methods for solving the Navier-Stokes equations. This formulation allows us to state classical and new numerical methods. Several examples are given. We combine them with finite element methods for spatial discretization. In particular, we propose two new second-order characteristics methods in terms of the displacement, one semi-Lagrangian and the other one pure Lagrangian. The pure Lagrangian displacement methods are useful for solving free surface problems and fluid-structure interaction problems because the computational domain is independent of the time and fluid-solid coupling at the interphase is straightforward. However, for moderate to high-Reynolds number flows, they can lead to high distortion in the mesh elements. When this happens it is necessary to remesh and reinitialize the transformation to the identity. In order to assess the performance of the obtained numerical methods, we solve different problems in two space dimensions. In particular, numerical results for a sloshing problem in a rectangular tank and the flow in a driven cavity are presented.

Keywords: Navier-Stokes equations, characteristics methods, Lagrange-Galerkin methods, second-order schemes, pure Lagrangian methods

1. Introduction

The main goal of the present paper is to introduce new second-order pure Lagrangian and semi-Lagrangian methods for the numerical solution of Navier-Stokes equations. In the scalar case, methods of characteristics for time discretization of convection-diffusion problems are extensively used (see the review paper [17]). These methods are based on time discretization of the material time derivative and were introduced in the beginning of the eighties of the last century combined with finite differences or finite elements for space discretization (see [14], [25]). When combined with finite elements they are also called Lagrange-Galerkin methods. In particular, when the characteristics methods are formulated in a fixed reference domain (respectively, in the current domain) they are called pure Lagrangian methods (respectively, semi-Lagrangian methods). In particular, the classical method of characteristics, as introduced in [14] and [25], is semi-Lagrangian and first order in time. There exists an extensive literature studying this characteristics method combined with finite elements applied to scalar convection-diffusion equations. If Δt denotes the time step, h the mesh-size and k the degree of the finite element space, estimates of the form $O(h^k)+O(\Delta t)$ in the $l^\infty(L^2(\mathbb{R}^d))$-norm are shown in [29] (d denotes the dimension of the spatial domain). Moreover, in [25] error estimates of the form $O(h^k)+O(\Delta t)+O(h^{k+1}/\Delta t)$ in the $l^\infty(L^2(\Omega))$-norm are obtained under the assumption that the normal velocity vanishes on the boundary of Ω. All of these estimates involve constants depending on solution norms. For linear finite elements and for a velocity field vanishing on the boundary, convergence of order $O(h^2)+O(\min(h,h^2/\Delta t))+O(\Delta t)$ in the $l^\infty(L^2(\Omega))$-norm is stated in [1], where the constants only depend on the data. In principle, the method of characteristics has been introduced for evolution equations but an adaption to solve stationary convection-diffusion problems has been proposed in [7].

Email addresses: marta.benitez@udc.es (M. Benítez), alfredo.bermudez@usc.es (A. Bermúdez)

In order to increase the order of time and space approximations, higher order schemes for the discretization of the material derivative and higher order finite element spaces should be used. In [27], a second-order characteristics method for solving constant coefficient convection-diffusion equations with Dirichlet boundary conditions is studied. The Crank-Nicholson discretization has been used to approximate the formulation involving the material time derivative. For a divergence-free velocity field vanishing on the boundary and a smooth enough solution, stability and $O(\Delta t^2) + O(h^k)$ error estimates in the $l^\infty(L^2(\Omega))$-norm are stated (see also [8] and [9] for further analysis).

Recently, for scalar linear convection-diffusion problems, we have introduced so-called pure Lagrangian methods combined with finite elements. In particular, in [4] and [5] $l^\infty(H^1(\Omega))$ stability and $l^\infty(H^1(\Omega))$ error estimates of order $O(\Delta t^2) + O(h^k)$ were proved for a second-order pure Lagrange-Galerkin method. Moreover, in [13], semi-Lagrangian and pure Lagrangian methods are proposed and analyzed for convection-diffusion equations. Error estimates for Galerkin discretization of a pure Lagrangian formulation and for a discontinuous Galerkin discretization of a semi-Lagrangian formulation are obtained. The estimates are written in terms of the projections constructed in [11] and [12]. In [4] and [5] a pure Lagrangian formulation has been used for more general problems. Specifically, we have considered a (possibly degenerate) variable coefficient diffusive term instead of the simpler Laplacian, general mixed Dirichlet-Robin boundary conditions, and a time dependent domain. Moreover, we have analyzed a scheme with approximate characteristic curves and presented numerical results for pure Lagrangian and semi-Lagrangian methods. In [2] a unified formulation to introduce Lagrangian and semi-Lagrangian methods for solving scalar linear convection-diffusion problems has been proposed and new stability estimates for the pure Lagrangian method proposed in [4] and [5] have been obtained. More precisely, an $l^\infty(H^1)-$stability estimate independent of the diffusion coefficient has been proved. Besides, if the given velocity field is incompressible, a stability inequality independent of the final time has been shown.

Usually, the unconditional stability of characteristics methods is only proved under the assumption that the inner products in the Galerkin formulation are exactly calculated. This is rarely possible so in practice they have to be calculated by using numerical quadrature. In general, this adds some terms to the final error estimates and, in some cases, it produces the loss of unconditional stability. There are several papers in the literature analyzing the effect of numerical integration in Lagrange-Galerkin methods (see [24], [29], [26], [19], [30], [9], [3]).

In this paper, we introduce a unified formulation to state pure Lagrangian and semi-Lagrangian methods for solving vector nonlinear convection-diffusion equations. More precisely, we are interested in solving the Navier-Stokes equations. For this purpose, we use the mathematical formalism of continuum mechanics (see for instance [22]) following the ideas given in [2].

The paper is organized as follows. In Section 2 the initial-boundary value problem to be solved is posed in a time dependent bounded domain and some hypotheses and notations concerning motions are stated. In Section 3, we introduce a quite general change of variable obtaining a new strong formulation of the problem. Moreover, the standard associated weak problem is obtained. In Section 4, semi-Lagrangian schemes in terms of the velocity are proposed. All these methods arise from the formulation obtained in the previous section. By using this formulation, in Section 5, two new Lagrange-Galerkin schemes in terms of the displacement are proposed, one pure Lagrangian and another one semi-Lagrangian. Finally, in Section 6 numerical examples are presented.

2. Statement of the nonlinear convection diffusion problem. General assumptions and notations

Let Ω be a bounded domain in $\mathbb{R}^d$ $(d = 2, 3)$ with Lipschitz boundary Γ divided into two parts: $\Gamma = \Gamma^D \cup \Gamma^N$, with $\Gamma^D \cap \Gamma^N = \emptyset$. Let t_0 and T be two non-negative constants and $X : \overline{\Omega} \times [t_0, T] \longrightarrow \mathbb{R}^d$ be a *motion* in the sense of Gurtin [22]. In particular, $X \in \mathbf{C}^3(\overline{\Omega} \times [t_0, T])$ and for each fixed $t \in [t_0, T]$, $X(\cdot, t)$ is a one-to-one function satisfying

$$\det F(p, t) > 0 \quad \forall p \in \overline{\Omega}, \tag{1}$$

being $F(\cdot, t)$ the *deformation gradient* of $X(\cdot, t)$. We call $\Omega_t = X(\Omega, t)$, $\Gamma_t = X(\Gamma, t)$, $\Gamma_t^D = X(\Gamma^D, t)$ and $\Gamma_t^N = X(\Gamma^N, t)$, for $t \in [t_0, T]$. We assume that $\Omega_{t_0} = \Omega$. Let us introduce the *trajectory* of the motion

$$\mathcal{T} := \{(x, t) : x \in \overline{\Omega}_t,\ t \in [t_0, T]\}.$$

For each t, $X(\cdot,t)$ is a one-to-one mapping from $\overline{\Omega}$ onto $\overline{\Omega}_t$; hence it has an inverse

$$P(\cdot,t) : \overline{\Omega}_t \longrightarrow \overline{\Omega}, \tag{2}$$

such that

$$X(P(x,t),t) = x, \qquad P(X(p,t),t) = p \quad \forall (x,t) \in \mathcal{T}\ \forall (p,t) \in \overline{\Omega} \times [t_0,T]. \tag{3}$$

The mapping $P : \mathcal{T} \longrightarrow \overline{\Omega}$, so defined is called the *reference map* of motion X and $P \in \mathbf{C}^3(\mathcal{T})$ (see [22] pp. $65-66$). We denote by p the *material points* in $\overline{\Omega}$, by t the *current time*, by x the *spatial points* in $\overline{\Omega}_t$ with $t > t_0$ and by y the points in $\overline{\Omega}_\tau$ with $\tau \leq T$. Besides, fields defined in $\mathcal{T}$ are called *spatial fields*. If Ψ is a spatial field, $\dot{\Psi}$ denotes the *material time derivative*, that is $\dot{\Psi}(x,t) = \dfrac{\partial}{\partial t}\left(\Psi(X(p,t),t)\right)_{|p=P(x,t)}$. Let us recall that the *spatial description* of the velocity $\mathbf{v} : \mathcal{T} \longrightarrow \mathbb{R}^d$ is defined by

$$\mathbf{v}(x,t) := \dot{X}(P(x,t),t) \quad \forall (x,t) \in \mathcal{T}, \tag{4}$$

being $\dot{X}$ the partial derivative of X with respect to the second argument (time).

Let us consider the following initial-boundary value problem.

(SP) **STRONG PROBLEM**. *Find two functions* $\mathbf{v} : \mathcal{T} \longrightarrow \mathbb{R}^d$ *and* $\pi : \mathcal{T} \longrightarrow \mathbb{R}$ *such that*

$$\begin{aligned} \rho(x,t)\frac{\partial \mathbf{v}}{\partial t}(x,t) + \rho(x,t)\,\mathrm{grad}\,\mathbf{v}(x,t)\mathbf{v}(x,t) \\ -\,\mathrm{div}\,\left\{-\pi(x,t)I + \mu(x,t)(\,\mathrm{grad}\,\mathbf{v}(x,t) + \,\mathrm{grad}\,\mathbf{v}^t(x,t))\right\} = \mathbf{b}(x,t), \end{aligned} \tag{5}$$

$$\mathrm{div}\,\mathbf{v}(x,t) = g(x,t), \tag{6}$$

for $x \in \Omega_t$ *and* $t \in (t_0,T)$, *subject to the boundary conditions*

$$\mathbf{v}(x,t) = \mathbf{v}_D(x,t) \text{ on } \Gamma_t^D, \tag{7}$$

$$\left(-\pi(x,t)I + \mu(x,t)(\,\mathrm{grad}\,\mathbf{v}(x,t) + \,\mathrm{grad}\,\mathbf{v}^t(x,t))\right)\mathbf{n}(x,t) = \mathbf{h}(x,t) \text{ on } \Gamma_t^N, \tag{8}$$

for $t \in (t_0,T)$, *and the initial condition*

$$\mathbf{v}(x,t_0) = \mathbf{v}^0(x) \text{ in } \Omega. \tag{9}$$

In the above equations, $\rho : \mathcal{T} \longrightarrow \mathbb{R}$, $\mu : \mathcal{T} \longrightarrow \mathbb{R}$, $\mathbf{b} : \mathcal{T} \longrightarrow \mathbb{R}^d$, $g : \mathcal{T} \longrightarrow \mathbb{R}$, $\mathbf{v}^0 : \Omega \longrightarrow \mathbb{R}^d$, $\mathbf{v}_D(\cdot,t) : \Gamma_t^D \longrightarrow \mathbb{R}^d$ and $\mathbf{h}(\cdot,t) : \Gamma_t^N \longrightarrow \mathbb{R}^d$, $t \in (t_0,T)$, are given spatial fields, I is the identity second order tensor and $\mathbf{n}(\cdot,t)$ is the outward unit normal vector to Γ_t. Let us notice that for $g = 0$ the above equations are the incompressible Navier-Stokes equations. Otherwise, they arise when modelling low-Mach number flows as those arising in many gas combustion problems. In this case function g is obtained from the mass conservation equation and the state law of the gas mixture as a function of temperature which, in its turn, is computed by solving the energy conservation equation.

For given $\tau \leq T$, motion X can also be defined relative to the configuration at time τ. It is the mapping

$$X_\tau : \quad \overline{\Omega}_\tau \times [t_0,T] \quad \longrightarrow \quad \mathbb{R}^d,$$

given by

$$X_\tau(y,t) := X(P(y,\tau),t) \quad \forall (y,t) \in \overline{\Omega}_\tau \times [t_0,T]. \tag{10}$$

Thus, mapping $t \in (t_0,T) \to X_\tau(y,t)$ represents the trajectory described by a material point that is at position y at time τ. Moreover, we notice that $x = X_\tau(y,t)$ if and only if $y = X_t(x,\tau)$. If Ψ is a spatial field, we introduce the field Ψ_τ, defined in $\overline{\Omega}_\tau \times [t_0,T]$ by

$$\Psi_\tau(y,t) := \Psi(X_\tau(y,t),t) \quad \forall (y,t) \in \overline{\Omega}_\tau \times [t_0,T]. \tag{11}$$

These functions are depicted in Figure 1. Notice that for $\tau = t$

$$\Psi_t(x,t) := \Psi(X_t(x,t),t) = \Psi(X(P(x,t),t),t) = \Psi(x,t).$$

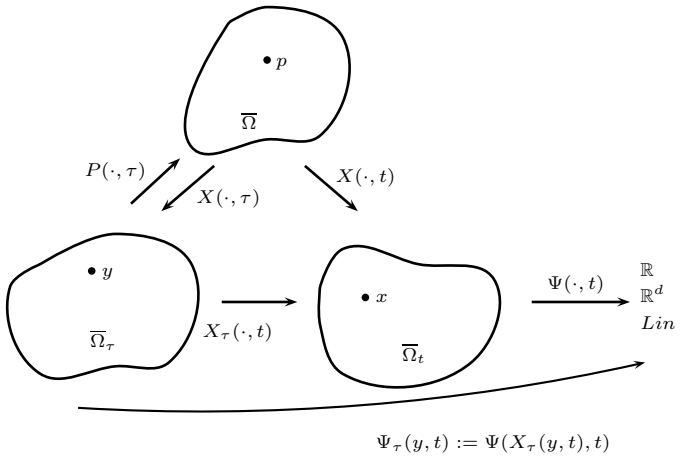

Figure 1: Functions referred to configuration at time $\tau \leq T$.

Let us introduce the displacement field relative to the configuration at time τ, that is,

$$\mathbf{u}_\tau(y,t) := X_\tau(y,t) - y \quad \forall (y,t) \in \overline{\Omega}_\tau \times [t_0, T]. \tag{12}$$

In the following $\mathcal{A}$ denotes a bounded domain in $\mathbb{R}^d$. Let us recall the definition of the Hilbert spaces $H^1(\mathcal{A})$ and $L^2(\mathcal{A})$:

$$L^2(\mathcal{A}) = \left\{ f : \mathcal{A} \longrightarrow \mathbb{R} \text{ measurable}, \ \int_\Omega f^2 dx < \infty \right\}, \tag{13}$$

$$H^1(\mathcal{A}) = \left\{ f : \mathcal{A} \longrightarrow \mathbb{R} \text{ measurable}, \ f, \ \frac{\partial f}{\partial x_i} \in L^2(\mathcal{A}), \ i = 1, \ldots, d \right\}. \tag{14}$$

We also introduce the notation $\mathbf{H}^1(\mathcal{A}) = \left(H^1(\mathcal{A})\right)^d$ and denote by $\mathbf{H}^1_{\Gamma^P}(\mathcal{A})$ the closed subspace of $\mathbf{H}^1(\mathcal{A})$ defined by

$$\mathbf{H}^1_{\Gamma^P}(\mathcal{A}) := \left\{ \mathbf{w} \in \mathbf{H}^1(\mathcal{A}), \ \mathbf{w}|_{\Gamma^P} \equiv 0 \right\}, \tag{15}$$

where Γ^P is a part of the boundary of $\mathcal{A}$ of non-null measure.

3. Strong problem and weak formulation in $\Omega_\tau \times (t_0, T)$

We are going to develop some formal computations in order to write the above problem (SP) in configuration Ω_τ, where $\tau \leq T$. First, from the definition of the material time derivative and by using the chain rule, we get

$$\dot{\mathbf{v}}(x,t) = \frac{\partial \mathbf{v}}{\partial t}(x,t) + \text{ grad}_x \mathbf{v}(x,t)\mathbf{v}(x,t) = \frac{\partial}{\partial t}\mathbf{v}_\tau(y,t)_{|y=X_t(x,\tau)} \ \forall (x,t) \in \mathcal{T}. \tag{16}$$

By using the above definitions, we have

$$\mathbf{v}_\tau(y,t) = \frac{\partial X_\tau}{\partial t}(y,t) = \frac{\partial \mathbf{u}_\tau}{\partial t}(y,t). \tag{17}$$

Then, from (16) and (17), we deduce

$$\frac{\partial \mathbf{v}}{\partial t}(x,t) + \text{ grad}_x \mathbf{v}(x,t)\mathbf{v}(x,t) = \frac{\partial^2 \mathbf{u}_\tau}{\partial t^2}(y,t)_{|y=X_t(x,\tau)} \ \forall (x,t) \in \mathcal{T}. \tag{18}$$

Next, by evaluating equations (5) and (6) at point $x = X_\tau(y,t)$ and then using (18), we obtain

$$\begin{aligned} \rho(X_\tau(y,t),t)\frac{\partial^2 \mathbf{u}_\tau}{\partial t^2}(y,t) - \text{ div}_x \{ -\pi(X_\tau(y,t),t)I \\ +\mu(X_\tau(y,t),t)(\text{ grad}_x \mathbf{v}(X_\tau(y,t),t) + \text{ grad}_x \mathbf{v}^t(X_\tau(y,t),t)) \} = \mathbf{b}(X_\tau(y,t),t), \end{aligned} \tag{19}$$

$$\text{div}_x \mathbf{v}(X_\tau(y,t),t) = g(X_\tau(y,t),t), \tag{20}$$

for $(y,t) \in \Omega_\tau \times (t_0,T)$. Note that in (19) and (20) there are derivatives with respect to the Eulerian variable x. In order to write a strong formulation of problem (SP) in coordinates $(y,t) \in \Omega_\tau \times (t_0,T)$ we use the divergence theorem, the change of variable $x = X_\tau(y,t)$ and the chain rule, to obtain the equalities

$$\begin{aligned} -\operatorname{div}_x \{-\pi(X_\tau(y,t),t)I + \mu(X_\tau(y,t),t)(\operatorname{grad}_x \mathbf{v}(X_\tau(y,t),t) + \operatorname{grad}_x \mathbf{v}^t(X_\tau(y,t),t))\} \\ = -\frac{1}{\det F_\tau(y,t)} \operatorname{div}_y \{(-\pi_\tau(y,t)I \\ + \mu_\tau(y,t)\left(\operatorname{grad}_y \frac{\partial \mathbf{u}_\tau}{\partial t}(y,t)F_\tau^{-1}(y,t) + F_\tau^{-t}(y,t)\left(\operatorname{grad}_y \frac{\partial \mathbf{u}_\tau}{\partial t}\right)^t (y,t)\right)\Big\} \det F_\tau(y,t) F_\tau^{-t}(y,t), \end{aligned} \tag{21}$$

$$\begin{aligned} \operatorname{div}_x \mathbf{v}(X_\tau(y,t),t) &= \operatorname{tr}(\operatorname{grad}_x \mathbf{v}(X_\tau(y,t),t)) = \operatorname{tr}\left(\operatorname{grad}_y \frac{\partial \mathbf{u}_\tau}{\partial t}(y,t)F_\tau^{-1}(y,t)\right) \\ &= \operatorname{grad}_y \frac{\partial \mathbf{u}_\tau}{\partial t}(y,t)F_\tau^{-1}(y,t) \cdot I = \operatorname{grad}_y \frac{\partial \mathbf{u}_\tau}{\partial t}(y,t) \cdot F_\tau^{-t}(y,t), \end{aligned} \tag{22}$$

for $(y,t) \in \Omega_\tau \times (t_0,T)$ and where we have used equality (17). Here and hereafter, the dot is used to denote the scalar product either of vectors or of second order tensors. Moreover, in the above equations, F_τ denotes the Jacobian matrix of the transformation X_τ. Next, by evaluating equations (7) and (8) at point $x = X_\tau(y,t)$ and equation (9) at point $P(y,\tau)$, and using (17), we obtain the following boundary and initial conditions for $\dfrac{\partial \mathbf{u}_\tau}{\partial t}$:

$$\begin{aligned} \frac{\partial \mathbf{u}_\tau}{\partial t}(y,t) = (\mathbf{v}_D)_\tau(y,t) \text{ on } \Gamma_\tau^D \times (t_0,T), \\ \left(-\pi_\tau(y,t)I + \mu_\tau(y,t)\left(\operatorname{grad}_y \frac{\partial \mathbf{u}_\tau}{\partial t}(y,t)F_\tau^{-1}(y,t) + F_\tau^{-t}(y,t)\left(\operatorname{grad}_y \frac{\partial \mathbf{u}_\tau}{\partial t}\right)^t (y,t)\right)\right) \\ F_\tau^{-t}(y,t)\mathbf{m}_\tau(y) = |F_\tau^{-t}(y,t)\mathbf{m}_\tau(y)|\mathbf{h}_\tau(y,t) \text{ on } \Gamma_\tau^N \times (t_0,T), \\ \frac{\partial \mathbf{u}_\tau}{\partial t}(y,t_0) = \mathbf{v}^0(P(y,\tau)) \text{ in } \overline{\Omega}_\tau, \end{aligned}$$

where $\mathbf{m}_\tau$ is the outward unit normal vector to $\partial\Omega_\tau$. The second condition has been obtained by using the chain rule and noting that

$$\mathbf{n}(X_\tau(y,t),t) = \frac{F_\tau^{-T}(y,t)\mathbf{m}_\tau(y)}{|F_\tau^{-T}(y,t)\mathbf{m}_\tau(y)|} \quad (y,t) \in \Gamma_\tau \times (t_0,T).$$

Thus, from these results, we deduce the following formulation in $\Omega_\tau \times (t_0,T)$ of the initial-boundary value problem (SP):

$(\mathrm{SP})_\tau$ **STRONG PROBLEM IN** $\Omega_\tau \times (t_0,T)$. *Find two functions* $\mathbf{u}_\tau : \overline{\Omega}_\tau \times [t_0,T] \longrightarrow \mathbb{R}^d$ *and* $\pi_\tau : \overline{\Omega}_\tau \times [t_0,T] \longrightarrow \mathbb{R}$ *such that*

$$\begin{aligned} \rho_\tau(y,t)\frac{\partial^2 \mathbf{u}_\tau}{\partial t^2}(y,t) - \frac{1}{\det F_\tau(y,t)} \operatorname{div}_y \Big\{ (-\pi_\tau(y,t)I \\ + \mu_\tau(y,t)\left(\operatorname{grad}_y \frac{\partial \mathbf{u}_\tau}{\partial t}(y,t)F_\tau^{-1}(y,t) + F_\tau^{-t}(y,t)\left(\operatorname{grad}_y \frac{\partial \mathbf{u}_\tau}{\partial t}\right)^t (y,t)\right)\Big\} \det F_\tau(y,t) F_\tau^{-t}(y,t) \\ = \mathbf{b}_\tau(y,t), \end{aligned} \tag{23}$$

$$\operatorname{grad}_y \frac{\partial \mathbf{u}_\tau}{\partial t}(y,t) \cdot F_\tau^{-t}(y,t) = g_\tau(y,t), \tag{24}$$

for $(y,t) \in \Omega_\tau \times (t_0,T)$*, subjected to the boundary conditions*

$$\frac{\partial \mathbf{u}_\tau}{\partial t}(y,t) = (\mathbf{v}_D)_\tau(y,t) \text{ on } \Gamma_\tau^D \times (t_0,T), \tag{25}$$

$$\begin{aligned}\left(-\pi_\tau(y,t)I + \mu_\tau(y,t)\left(\operatorname{grad}_y \frac{\partial \mathbf{u}_\tau}{\partial t}(y,t)F_\tau^{-1}(y,t) + F_\tau^{-t}(y,t)\left(\operatorname{grad}_y \frac{\partial \mathbf{u}_\tau}{\partial t}\right)^t(y,t)\right)\right)\\ F_\tau^{-t}(y,t)\mathbf{m}_\tau(y) = |F_\tau^{-t}(y,t)\mathbf{m}_\tau(y)|\mathbf{h}_\tau(y,t) \text{ on } \Gamma_\tau^N \times (t_0,T),\end{aligned} \tag{26}$$

and the initial condition

$$\frac{\partial \mathbf{u}_\tau}{\partial t}(y,t_0) = \mathbf{v}^0(P(y,\tau)) \text{ in } \overline{\Omega}_\tau. \tag{27}$$

Depending of the choice of τ, we can obtain different Lagrangian and semi-Lagrangian methods. More precisely, the *pure Lagrangian* methods (respectively, the *semi-Lagrangian* methods) are obtained when τ is fixed along the time integration, that is, it is independent of the current time t (respectively, when τ changes along the time integration, that is, it changes with t). Among semi-Lagrangian methods we can distinguish *forward* semi-Lagrangian (if $\tau < t$) and *backward* semi-Lagrangian (if $\tau > t$). Now, we are going to obtain a weak formulation of $(\mathrm{SP})_\tau$. Let us multiply (23) by $\det F_\tau$ and by a test function $\mathbf{z} \in \mathbf{H}^1_{\Gamma_\tau^D}(\Omega_\tau)$, integrate in Ω_τ, and apply the usual Green's formula and (26). Similarly, let us multiply (24) by $\det F_\tau$ and by a test function $q \in L^2(\Omega_\tau)$, and integrate in Ω_τ. We get

$$\begin{aligned}\int_{\Omega_\tau} \rho_\tau(y,t)\det F_\tau(y,t)\frac{\partial^2 \mathbf{u}_\tau}{\partial t^2}(y,t)\cdot \mathbf{z}(y)\,dy - \int_{\Omega_\tau} \pi_\tau(y,t)\det F_\tau(y,t)F_\tau^{-t}(y,t)\cdot \operatorname{grad}\mathbf{z}(y)\,dy\\ + \int_{\Omega_\tau} \mu_\tau(y,t)\left(\operatorname{grad}_y \frac{\partial \mathbf{u}_\tau}{\partial t}(y,t)F_\tau^{-1}(y,t) + F_\tau^{-t}(y,t)\left(\operatorname{grad}_y \frac{\partial \mathbf{u}_\tau}{\partial t}\right)^t(y,t)\right)\\ \det F_\tau(y,t)F_\tau^{-t}(y,t)\cdot \operatorname{grad}\mathbf{z}(y)\,dy = \int_{\Omega_\tau} \mathbf{b}_\tau(y,t)\cdot\mathbf{z}(y)\det F_\tau(y,t)\,dy\\ + \int_{\Gamma_\tau^N} |F_\tau^{-t}(y,t)\mathbf{m}_\tau(y)|\det F_\tau(y,t)\mathbf{h}_\tau(y,t)\cdot\mathbf{z}(y)\,dA_y,\end{aligned} \tag{28}$$

$$\int_{\Omega_\tau} \det F_\tau(y,t)\operatorname{grad}_y \frac{\partial \mathbf{u}_\tau}{\partial t}(y,t)\cdot F_\tau^{-t}(y,t)q(y)\,dy = \int_{\Omega_\tau} \det F_\tau(y,t)g_\tau(y,t)q(y)\,dy, \tag{29}$$

$\forall \mathbf{z} \in \mathbf{H}^1_{\Gamma_\tau^D}(\Omega_\tau)$, $\forall q \in L^2(\Omega_\tau)$ and $t \in (t_0,T)$. These are formal computations, i.e., we have assumed appropriate regularity of the involved data and solution.

Remark 3.1. *Notice that equations (28)-(29) can also be written in terms of the velocity instead of the displacement, by replacing* $\dfrac{\partial \mathbf{u}_\tau}{\partial t}(y,t)$ *with* $\mathbf{v}_\tau(y,t)$*. Thus, from (28)-(29) we can obtain Lagrangian and semi-Lagrangian methods in terms of either the velocity or the displacement. We will call* velocity methods *(respectively,* displacement methods*) to those written in terms of the velocity (respectively, of the displacement). The classical characteristics methods for Navier-Stokes equations are semi-Lagrangian velocity schemes. In the next sections, we are going to obtain, from (28)-(29), different characteristics methods, in particular the classical ones.*

4. Time discretization: characteristics methods in terms of velocity

In this section, we present semi-Lagrangian velocity methods. They are obtained by introducing different time semi-discretizations of problem $(\mathrm{SP})_\tau$ written in terms of $\mathbf{v}_\tau(y,t)$ instead of $\dfrac{\partial \mathbf{u}_\tau}{\partial t}(y,t)$.

Remark 4.1. *Notice that* $X_\tau(y,t)$ *and* $F_\tau(y,t)$ *appearing in (28)-(29) are unknown; but they can be approximated by using an approximation of either the velocity or the displacement.*

- *Displacement methods. For these methods, approximations of* X_τ *and* F_τ *can be easily obtained by using the following equalities:*

$$\begin{aligned}X_\tau(y,t) &= y + \mathbf{u}_\tau(y,t),\\ F_\tau(y,t) &= \operatorname{grad} X_\tau(y,t) = I + \operatorname{grad}\mathbf{u}_\tau(y,t).\end{aligned}$$

- *Velocity methods. For these methods, we can observe that X_τ and F_τ are the solutions to the following initial-value problems of ordinary differential equations (y is arbitrarily taken but fixed):*

$$\begin{aligned}\frac{\partial X_\tau}{\partial t}(y,t) &= \mathbf{v}_\tau(y,t) \quad X_\tau(y,\tau) = y,\\ \frac{\partial F_\tau}{\partial t}(y,t) &= \operatorname{grad}_y \mathbf{v}_\tau(y,t) \quad F_\tau(y,\tau) = I,\end{aligned}$$

being $y \in \Omega_\tau$. Then, approximations of X_τ and F_τ can be obtained by using numerical methods to solve these initial-value problems.

The following notations will be used in the rest of the paper. Let us introduce the number of time steps, N, the time step $\Delta t = (T - t_0)/N$, and the mesh-points $t_n = t_0 + n\Delta t$.

Depending on the values of τ and t, on the differentiation formulas used to approximate the time derivatives and on the numerical formulas used to approximate the other terms, we can obtain different characterictics methods. Let Ψ be a spatial field. We will use the following notation:

$$\Psi_j^l(y) := \Psi_{t_j}(y, t_l)\ \forall y \in \Omega_{t_j}, \quad \forall j, l. \tag{30}$$

In particular, for $j = l$ we will simply write Ψ^l instead of Ψ_l^l. Let us notice that $F_l^l = I\ \forall\, l$.

Similarly, in what follows we will denote by $\Psi_{j,\Delta t}^l$ (respectively, $\Psi_{j,\Delta t,h}^l$) approximations of Ψ_j^l obtained with a time semidiscretized scheme (respectively, a fully discretized scheme).

- *One-step semi-Lagrangian schemes*: This one-parameter family of methods arises from fixing $\tau = t_{n+1}$, $t = t_{n+\theta}$ in (23) and $t = t_{n+1}$ in (24), and using a two-point formula to approximate $\dfrac{\partial \mathbf{v}_\tau}{\partial t}$ and a convex linear combination involving the values at $t = t_n$ and $t = t_{n+1}$ to approximate the rest of the terms at time $t_{n+\theta}$. More precisely:

$$\begin{aligned}&(\theta\rho^{n+1}(x) + (1-\theta)\rho_{n+1,\Delta t}^n(x))\frac{\mathbf{v}_{\Delta t}^{n+1}(x) - \mathbf{v}_{n+1,\Delta t}^n(x)}{\Delta t}\\ &-\theta \operatorname{div}\left\{\left(-\pi_{\Delta t}^{n+1}(x)I + \mu^{n+1}(x)\left(\operatorname{grad}\mathbf{v}_{\Delta t}^{n+1}(x) + \left(\operatorname{grad}\mathbf{v}_{\Delta t}^{n+1}(x)\right)^t(x)\right)\right)\right\}\\ &-(1-\theta)\frac{1}{\det F_{n+1,\Delta t}^n(x)}\operatorname{div}\left\{\left(-\pi_{n+1,\Delta t}^n(x)I + \mu_{n+1,\Delta t}^n(x)\left(\operatorname{grad}\mathbf{v}_{n+1,\Delta t}^n(x)\right.\right.\right.\\ &\left.\left.\left.(F_{n+1,\Delta t}^n)^{-1}(x) + (F_{n+1,\Delta t}^n)^{-t}(x)\left(\operatorname{grad}\mathbf{v}_{n+1,\Delta t}^n\right)^t(x)\right)\right)\det F_{n+1,\Delta t}^n(x)(F_{n+1,\Delta t}^n)^{-t}(x)\right\}\\ &= \theta\mathbf{b}^{n+1}(x) + (1-\theta)\mathbf{b}_{n+1,\Delta t}^n(x),\ x \in \Omega_{t_{n+1}},\end{aligned} \tag{31}$$

$$\operatorname{div}\mathbf{v}_{\Delta t}^{n+1}(x) = g^{n+1}(x),\ x \in \Omega_{t_{n+1}}, \tag{32}$$

for $0 \le n \le N-1$.

Particular cases:

1. When $\theta = 1$, we obtain the classical first order semi-Lagrangian scheme proposed in [25].
2. When $\theta = 1/2$, we obtain a new second-order semi-Lagrangian scheme similar to the one analyzed in [8] and [9] for linear scalar convection-diffusion problems.

- *Two-step second-order semi-Lagrangian scheme*: This method has been proposed in [10] for the incompressible Navier-Stokes equations. It can be introduced in our framework by taking $\tau = t_{n+1}$, $t = t_{n+1}$, and using the following second-order backward formula to approximate $\dfrac{\partial \mathbf{v}_\tau}{\partial t}$:

$$\frac{\partial \mathbf{v}_\tau}{\partial t}(y,t) = \frac{1}{2\Delta t}(3\mathbf{v}_\tau(y,t) - 4\mathbf{v}_\tau(y,t-\Delta t) + \mathbf{v}_\tau(y,t-2\Delta t)) + O(\Delta t^2). \tag{33}$$

More precisely:

$$\rho^{n+1}(x)\frac{3\mathbf{v}_{\Delta t}^{n+1}(x)-4\mathbf{v}_{n+1,\Delta t}^{n}(x)+\mathbf{v}_{n+1,\Delta t}^{n-1}(x)}{2\Delta t}$$
$$-\operatorname{div}\left\{\left(-\pi_{\Delta t}^{n+1}(x)I+\mu^{n+1}(x)\left(\operatorname{grad}\mathbf{v}_{\Delta t}^{n+1}(x)+\left(\operatorname{grad}\mathbf{v}_{\Delta t}^{n+1}(x)\right)^{t}(x)\right)\right)\right\} \tag{34}$$
$$=\mathbf{b}^{n+1}(x),\ x\in\Omega_{t_{n+1}},$$
$$\operatorname{div}\mathbf{v}_{\Delta t}^{n+1}(x)=g^{n+1}(x),\ x\in\Omega_{t_{n+1}}, \tag{35}$$

where $1\leq n\leq N-1$. In [3] this method has been applied to solve natural convection problems.

Remark 4.2. *In the above methods, the characteristics curves and their gradients are approximated by using the procedures given in Remark 4.1. Notice that F does not appear either in the classical first order semi-Lagrangian scheme or in the two-step second-order semi-Lagrangian scheme. However, for both methods, in order to calculate $\mathbf{v}_{n+1,\Delta t}^{l}$, it is necessary to obtain an approximation of the characteristics curves X_{n+1}^{l}, being $l=n$ for the classical method and $l=n,n-1$ for the second-order one (see [3] for further details).*

5. New characteristics methods in terms of the displacement

In order to obtain characteristics methods in terms of the displacement, we consider the following formulas to approximate the time derivatives $\dfrac{\partial^2\mathbf{u}_\tau}{\partial t^2}(y,t)$ and $\dfrac{\partial\mathbf{u}_\tau}{\partial t}(y,t)$:

- Three-point second-order centered formula:

$$\frac{\partial^2\mathbf{u}_\tau}{\partial t^2}(y,t)=\frac{\mathbf{u}_\tau(y,t+\Delta t)-2\mathbf{u}_\tau(y,t)+\mathbf{u}_\tau(y,t-\Delta t)}{\Delta t^2}+O(\Delta t^2). \tag{36}$$

- Two-point second-order centered formula:

$$\frac{\partial\mathbf{u}_\tau}{\partial t}(y,t)=\frac{\mathbf{u}_\tau(y,t+\Delta t)-\mathbf{u}_\tau(y,t-\Delta t)}{2\Delta t}+O(\Delta t^2). \tag{37}$$

5.1. Pure Lagrangian scheme

In this section we introduce a pure Lagrange-Galerkin scheme for fully discretization of (28)-(29). Firstly, we propose a second order pure Lagrangian scheme for time semi-discretization of (28)-(29). Next, we propose a space discretization of the time semidiscretized problem by using finite elements spaces.

5.1.1. Time discretization

By taking $\tau=t_0-\dfrac{\Delta t}{2}$ and $t=t_{n+1/2}$ in (28)-(29), and using the second-order formulas (36) and (37), we obtain the time-discretized scheme

$$\int_{\Omega_{t_0-\Delta t/2}}\rho^{n+1/2}\circ X_{-1/2,\Delta t}^{n+1/2}\det F_{-1/2,\Delta t}^{n+1/2}\frac{\mathbf{u}_{-1/2,\Delta t}^{n+3/2}-2\mathbf{u}_{-1/2,\Delta t}^{n+1/2}+\mathbf{u}_{-1/2,\Delta t}^{n-1/2}}{\Delta t^2}\cdot\mathbf{z}\,dy$$
$$-\int_{\Omega_{t_0-\Delta t/2}}\pi_{-1/2,\Delta t}^{n+1/2}\det F_{-1/2,\Delta t}^{n+1/2}(F_{-1/2,\Delta t}^{n+1/2})^{-t}\cdot\operatorname{grad}\mathbf{z}\,dy$$
$$+\int_{\Omega_{t_0-\Delta t/2}}\mu^{n+1/2}\circ X_{-1/2,\Delta t}^{n+1/2}\det F_{-1/2,\Delta t}^{n+1/2}\frac{\operatorname{grad}\mathbf{u}_{-1/2,\Delta t}^{n+3/2}-\operatorname{grad}\mathbf{u}_{-1/2,\Delta t}^{n-1/2}}{2\Delta t}$$
$$(F_{-1/2,\Delta t}^{n+1/2})^{-1}(F_{-1/2,\Delta t}^{n+1/2})^{-t}\cdot\operatorname{grad}\mathbf{z}\,dy+\int_{\Omega_{t_0-\Delta t/2}}\mu^{n+1/2}\circ X_{-1/2,\Delta t}^{n+1/2}\det F_{-1/2,\Delta t}^{n+1/2}(F_{-1/2,\Delta t}^{n+1/2})^{-t} \tag{38}$$
$$\frac{(\operatorname{grad}\mathbf{u}_{-1/2,\Delta t}^{n+3/2})^{t}-(\operatorname{grad}\mathbf{u}_{-1/2,\Delta t}^{n-1/2})^{t}}{2\Delta t}(F_{-1/2,\Delta t}^{n+1/2})^{-t}\cdot\operatorname{grad}\mathbf{z}\,dy$$
$$=\int_{\Omega_{t_0-\Delta t/2}}\det F_{-1/2,\Delta t}^{n+1/2}\mathbf{b}^{n+1/2}\circ X_{-1/2,\Delta t}^{n+1/2}\cdot\mathbf{z}\,dy$$

$$
\begin{aligned}
&+\int_{\Gamma^N_{t_0-\Delta t/2}} |(F^{n+1/2}_{-1/2,\Delta t})^{-t}\mathbf{m}_{t_0-\Delta t/2}|\det F^{n+1/2}_{-1/2,\Delta t}\mathbf{h}^{n+1/2}\circ X^{n+1/2}_{-1/2,\Delta t}\cdot\mathbf{z}\,dA_y,\\
&\int_{\Omega_{t_0-\Delta t/2}} \det F^{n+1/2}_{-1/2,\Delta t}\frac{\operatorname{grad}\mathbf{u}^{n+3/2}_{-1/2,\Delta t}-\operatorname{grad}\mathbf{u}^{n-1/2}_{-1/2,\Delta t}}{2\Delta t}\cdot(F^{n+1/2}_{-1/2,\Delta t})^{-t}q\,dy\\
&\qquad=\int_{\Omega_{t_0-\Delta t/2}}\det F^{n+1/2}_{-1/2,\Delta t}g^{n+1/2}\circ X^{n+1/2}_{-1/2,\Delta t}q\,dy,
\end{aligned}
\tag{39}
$$

$\forall\mathbf{z}\in\mathbf{H}^1_{\Gamma^D_{t_0-\Delta t/2}}(\Omega_{t_0-\Delta t/2})$, $\forall q\in L^2(\Omega_{t_0-\Delta t/2})$ and $0\le n\le N-1$. In the above pure Lagrangian problem, we have used the following notations

$$
\begin{aligned}
X^{n+1/2}_{-1/2,\Delta t}(y)&:=y+\mathbf{u}^{n+1/2}_{-1/2,\Delta t}(y),\\
F^{n+1/2}_{-1/2,\Delta t}(y)&:=I+\operatorname{grad}\mathbf{u}^{n+1/2}_{-1/2,\Delta t}(y),
\end{aligned}
$$

for $y\in\Omega_{t_0-\Delta t/2}$ and $0\le n\le N-1$. Notice that problem (38)-(39) is linear in the unknowns $\mathbf{u}^{n+3/2}_{-1/2,\Delta t}$ and $\pi^{n+1/2}_{-1/2,\Delta t}$.

In general, $\Omega_{t_0-\Delta t/2}$ is unknown; instead we calculate an approximation by using the following second order approximation of the motion:

$$
X_{\Delta t}(p,t_{0-\Delta t/2})=p-\mathbf{v}^0(p)\frac{\Delta t}{2},
$$

for $p\in\Omega$.

Remark 5.1. *In order to obtain the initial conditions for the pure Lagrangian method (38)-(39), we observe that* $\mathbf{u}^{-1/2}_{-1/2}(y):=\mathbf{u}_{-1/2}(y,t_0-\Delta t/2)=\mathbf{0}\ \forall y\in\overline{\Omega}_{t_0-\Delta t/2}$. *Moreover, a third order approximation of* $\mathbf{u}^{1/2}_{-1/2}$ *can be obtained by using (27), namely*

$$
\mathbf{u}^{1/2}_{-1/2}(y)=\Delta t\mathbf{v}^0\left(y+\mathbf{v}^0(y)\frac{\Delta t}{2}\right)+O(\Delta t^3)\simeq\Delta t\mathbf{v}^0\left(y+\mathbf{v}^0(y)\frac{\Delta t}{2}\right),
$$

where we have used that $\mathbf{u}_{-1/2}(y,t_0-\Delta t/2)=\mathbf{0}$. *Then we take*

$$
\mathbf{u}^{1/2}_{-1/2,\Delta t}(y):=\Delta t\mathbf{v}^0\left(y+\mathbf{v}^0(y)\frac{\Delta t}{2}\right).
$$

In the academic test examples, we have observed that for the above method to be second-order in time for the velocity it is necessary to start with a third order approximation of $\mathbf{u}^{1/2}_{-1/2}$ *as the previous one.*

Remark 5.2. *By using analogous procedures to the ones in Remark 5.1, we can obtain approximate Dirichlet boundary conditions for the displacement. More precisely, by using that*

$$
\mathbf{u}^{n+3/2}_{-1/2}(y)=\mathbf{u}^{n+1/2}_{-1/2}(y)+\Delta t\mathbf{v}^{n+1}\left(X_{-1/2}(y,t_{n-1/2})+\mathbf{v}^{n-1/2}(X_{-1/2}(y,t_{n-1/2}))\frac{3}{2}\Delta t\right)+O(\Delta t^3),
$$

we deduce the following Dirichlet boundary condition for $\mathbf{u}^{n+3/2}_{-1/2}$*:*

$$
\mathbf{u}^{n+3/2}_{-1/2,\Delta t}(y)=\mathbf{u}^{n+1/2}_{-1/2,\Delta t}(y)+\Delta t\mathbf{v}^{n+1}_D\left(X^{n-1/2}_{-1/2,\Delta t}(y)+\mathbf{v}^{n-1/2}_D(X^{n-1/2}_{-1/2,\Delta t}(y))\frac{3}{2}\Delta t\right)\ \text{ on }\Gamma^D_{t_0-\Delta t/2}.
$$

5.1.2. Space discretization. Finite element method

We propose a space discretization of the above problem by using continuous piecewise-linear+bubble finite element for each displacement component and continuous piecewise-linear for pressure.

Let us suppose $\Omega_{t_0-\Delta t/2}$ is a bounded domain in $\mathbb{R}^d$ with a Lipschitz polygonal boundary. Let us consider a suitable family of regular triangulations of $\overline{\Omega}_{t_0-\Delta t/2}$ to be denoted by $\mathfrak{T}_h$, consisting of elements

K of diameter $\leq h$. Moreover, we assume it is compatible with the partition of the boundary into $\Gamma^D_{t_0-\Delta t/2}$ and $\Gamma^N_{t_0-\Delta t/2}$.

We define the following polynomial spaces:

$$P_1(K) = \left\{ q_{|K} : q : \mathbb{R}^d \longrightarrow \mathbb{R} \text{ polynomial of degree } \leq 1 \right\},$$
$$P_b(K) = \left\{ q + \alpha \lambda_b^K : q \in P_1(K) \ , \ \alpha \in \mathbb{R} \right\},$$

where λ_b^K is the bubble function of element K.
We consider the following spaces of finite elements:

$$X_h = \left\{ \mathbf{w}_h \in \left(C^0(\Omega_{t_0-\Delta t/2}) \right)^d : \ \mathbf{w}_{h|K} \in (P_b(K))^d, \quad \forall K \in \mathfrak{T}_h \right\}, \tag{40}$$

$$X_{0h} = \left\{ \mathbf{w}_h \in X_h : \ \mathbf{w}_h = \mathbf{0} \text{ on } \Gamma^D_{t_0-\Delta t/2} \right\}, \tag{41}$$

$$V_h = \left\{ \varphi_h \in C^0(\Omega_{t_0-\Delta t/2}) : \ \varphi_{h|K} \in P_1(K), \quad \forall K \in \mathfrak{T}_h \right\}. \tag{42}$$

In order to obtain fully discrete scheme of the time semidiscretizated problem (38)-(39) we use the approximations of function spaces $\mathbf{H}^1(\Omega_{t_0-\Delta t/2})$, $\mathbf{H}^1_{\Gamma^D_{t_0-\Delta t/2}}(\Omega_{t_0-\Delta t/2})$ and $L^2(\Omega_{t_0-\Delta t/2})$ given by (40), (41) and (42), respectively.
Thus, we obtain the following fully discrete problem:

(**LG**).– Find two sequences of functions $\widehat{\mathbf{u}}_{-1/2,\Delta t,h} = \{\mathbf{u}^{n+3/2}_{-1/2,\Delta t,h}\}_{n=0}^{N-1} \in [X_h]^N$ and $\widehat{\pi}_{-1/2,\Delta t,h} = \{\pi^{n+1/2}_{-1/2,\Delta t,h}\}_{n=0}^{N-1} \in [V_h]^N$ such that

$$\begin{aligned}
&\int_{\Omega_{t_0-\Delta t/2}} \rho^{n+1/2} \circ X^{n+1/2}_{-1/2,\Delta t,h} \det F^{n+1/2}_{-1/2,\Delta t,h} \frac{\mathbf{u}^{n+3/2}_{-1/2,\Delta t,h} - 2\mathbf{u}^{n+1/2}_{-1/2,\Delta t,h} + \mathbf{u}^{n-1/2}_{-1/2,\Delta t,h}}{\Delta t^2} \cdot \mathbf{z}_h \, dy \\
&\qquad - \int_{\Omega_{t_0-\Delta t/2}} \pi^{n+1/2}_{-1/2,\Delta t,h} \det F^{n+1/2}_{-1/2,\Delta t,h} (F^{n+1/2}_{-1/2,\Delta t,h})^{-t} \cdot \operatorname{grad} \mathbf{z}_h \, dy \\
&\qquad + \int_{\Omega_{t_0-\Delta t/2}} \mu^{n+1/2} \circ X^{n+1/2}_{-1/2,\Delta t,h} \det F^{n+1/2}_{-1/2,\Delta t,h} \frac{\operatorname{grad} \mathbf{u}^{n+3/2}_{-1/2,\Delta t,h} - \operatorname{grad} \mathbf{u}^{n-1/2}_{-1/2,\Delta t,h}}{2\Delta t} \\
&\qquad\qquad (F^{n+1/2}_{-1/2,\Delta t,h})^{-1} (F^{n+1/2}_{-1/2,\Delta t,h})^{-t} \cdot \operatorname{grad} \mathbf{z}_h \, dy \\
&\qquad + \int_{\Omega_{t_0-\Delta t/2}} \mu^{n+1/2} \circ X^{n+1/2}_{-1/2,\Delta t,h} \det F^{n+1/2}_{-1/2,\Delta t,h} (F^{n+1/2}_{-1/2,\Delta t,h})^{-t} \\
&\qquad\qquad \frac{(\operatorname{grad} \mathbf{u}^{n+3/2}_{-1/2,\Delta t,h})^t - (\operatorname{grad} \mathbf{u}^{n-1/2}_{-1/2,\Delta t,h})^t}{2\Delta t} (F^{n+1/2}_{-1/2,\Delta t,h})^{-t} \cdot \operatorname{grad} \mathbf{z}_h \, dy \\
&\qquad = \int_{\Omega_{t_0-\Delta t/2}} \det F^{n+1/2}_{-1/2,\Delta t,h} \mathbf{b}^{n+1/2} \circ X^{n+1/2}_{-1/2,\Delta t,h} \cdot \mathbf{z}_h \, dy \\
&+ \int_{\Gamma^N_{t_0-\Delta t/2}} |(F^{n+1/2}_{-1/2,\Delta t,h})^{-t} \mathbf{m}_{t_0-\Delta t/2}| \det F^{n+1/2}_{-1/2,\Delta t,h} \mathbf{h}^{n+1/2} \circ X^{n+1/2}_{-1/2,\Delta t,h} \cdot \mathbf{z}_h \, dA_y, \ \forall \mathbf{z}_h \in X_{0h}
\end{aligned} \tag{43}$$

$$\begin{aligned}
&\int_{\Omega_{t_0-\Delta t/2}} \det F^{n+1/2}_{-1/2,\Delta t,h} \frac{\operatorname{grad} \mathbf{u}^{n+3/2}_{-1/2,\Delta t,h} - \operatorname{grad} \mathbf{u}^{n-1/2}_{-1/2,\Delta t,h}}{2\Delta t} \cdot (F^{n+1/2}_{-1/2,\Delta t,h})^{-t} q_h \, dy \\
&\qquad = \int_{\Omega_{t_0-\Delta t/2}} \det F^{n+1/2}_{-1/2,\Delta t,h} g^{n+1/2} \circ X^{n+1/2}_{-1/2,\Delta t,h} q_h \, dy, \ \forall q_h \in V_h,
\end{aligned} \tag{44}$$

for $0 \leq n \leq N-1$, with

$$\mathbf{u}^{-1/2}_{-1/2,\Delta t,h}(y) = \mathbf{0}, \text{ for all node } y \text{ of mesh } \mathfrak{T}_h, \tag{45}$$

$$\mathbf{u}^{1/2}_{-1/2,\Delta t,h}(y) = \Delta t \mathbf{v}^0\left(y + \mathbf{v}^0(y)\frac{\Delta t}{2}\right), \text{ for all node } y \text{ of mesh } \mathfrak{T}_h, \tag{46}$$

$$\begin{aligned}\mathbf{u}^{n+3/2}_{-1/2,\Delta t,h}(y) = \mathbf{u}^{n+1/2}_{-1/2,\Delta t,h}(y) + \Delta t \mathbf{v}^{n+1}_D\left(X^{n-1/2}_{-1/2,\Delta t,h}(y) + \mathbf{v}^{n-1/2}_D(X^{n-1/2}_{-1/2,\Delta t,h}(y))\frac{3}{2}\Delta t\right)\\ \text{for all node } y \text{ on } \Gamma^D_{t_0-\Delta t/2},\end{aligned} \tag{47}$$

and where $X^{n+1/2}_{-1/2,\Delta t,h}(y) = y + \mathbf{u}^{n+1/2}_{-1/2,\Delta t,h}(y)$, $F^{n+1/2}_{-1/2,\Delta t,h|K} = I + \operatorname{grad}\mathbf{u}^{n+1/2}_{-1/2,\Delta t,h|K}$ for $y \in \Omega_{t_0-\Delta t/2}$, $K \in \mathfrak{T}_h$ and $0 \leq n \leq N-1$.

By using the solution of problem (**LG**), we can obtain approximations of the followings fields: the velocity relative to $\Omega_{t_0-\Delta t/2}$ at times $\{t_{n+1}\}_{n=0}^{N-1}$, the velocity in Eulerian coordinates at times $\{t_{n+1}\}_{n=0}^{N-1}$, the motion relative to $\Omega_{t_0-\Delta t/2}$ at times $\{t_{n+1}\}_{n=0}^{N-1}$ and the pressure in Eulerian coordinates at times $\{t_{n+1/2}\}_{n=0}^{N-1}$. These approximations will be denoted respectively by $\{\mathbf{v}^{n+1}_{-1/2,\Delta t,h}\}_{n=0}^{N-1}$, $\{\mathbf{v}^{n+1}_{\Delta t,h}\}_{n=0}^{N-1}$, $\{X^{n+1}_{-1/2,\Delta t,h}\}_{n=0}^{N-1}$ and $\{\pi^{n+1/2}_{\Delta t,h}\}_{n=0}^{N-1}$.

- **Approximate velocity relative to $\Omega_{t_0-\Delta t/2}$.** It can be easily obtained by using (17) and a second-order centered formula to approximate $\dfrac{\partial \mathbf{u}_{-1/2}}{\partial t}$. More precisely, since

$$\mathbf{v}^{n+1}_{-1/2}(y) = \left(\frac{\partial \mathbf{u}_{-1/2}}{\partial t}\right)(y, t_{n+1}) = \frac{\mathbf{u}^{n+3/2}_{-1/2}(y) - \mathbf{u}^{n+1/2}_{-1/2}(y)}{\Delta t} + O(\Delta t^2)$$

  we define

$$\mathbf{v}^{n+1}_{-1/2,\Delta t,h}(y) := \frac{\mathbf{u}^{n+3/2}_{-1/2,\Delta t,h}(y) - \mathbf{u}^{n+1/2}_{-1/2,\Delta t,h}(y)}{\Delta t},$$

  for $y \in \Omega_{t_0-\Delta t/2}$ and $0 \leq n \leq N-1$.

- **Motion approximation relative to $\Omega_{t_0-\Delta t/2}$ at times $\{t_{n+1}\}_{n=0}^{N-1}$.** Noting that $\mathbf{u}_{-1/2}(y,t) = X_{-1/2}(y,t) - y$ and using a second-order centered formula, we obtain

$$X^{n+1}_{-1/2}(y) = y + \frac{\mathbf{u}^{n+3/2}_{-1/2}(y) + \mathbf{u}^{n+1/2}_{-1/2}(y)}{2} + O(\Delta t^2).$$

  Then we define the approximation

$$X^{n+1}_{-1/2,\Delta t,h}(y) := y + \frac{\mathbf{u}^{n+3/2}_{-1/2,\Delta t,h}(y) + \mathbf{u}^{n+1/2}_{-1/2,\Delta t,h}(y)}{2},$$

  for $y \in \Omega_{t_0-\Delta t/2}$ and $0 \leq n \leq N-1$.

- **Approximate velocity in Eulerian coordinates.** Let us denote by $\{y^h_i\}_{i=1}^{N^h_v}$ the vertices of mesh $\mathfrak{T}_h$. In order to obtain an approximate velocity in Eulerian coordinates, we consider this as a piecewise linear function on the moved mesh $\widetilde{\mathfrak{T}}^{n+1}_h$, being $\{X^{n+1}_{-1/2,\Delta t,h}(y^h_i)\}_{i=1}^{N^h_v}$ the vertices of this mesh. The values of $\mathbf{v}^{n+1}_{\Delta t,h}$ at vertices $\{X^{n+1}_{-1/2,\Delta t,h}(y^h_i)\}_{i=1}^{N^h_v}$, can be obtained by using $\mathbf{v}^{n+1}_{-1/2,\Delta t,h}$. Since we have

$$\mathbf{v}^{n+1}(X^{n+1}_{-1/2,\Delta t,h}(y^h_i)) \simeq \mathbf{v}^{n+1}(X^{n+1}_{-1/2}(y^h_i)) = \mathbf{v}^{n+1}_{-1/2}(y^h_i) \simeq \mathbf{v}^{n+1}_{-1/2,\Delta t,h}(y^h_i),$$

  we take the approximation

$$\mathbf{v}^{n+1}_{\Delta t,h}(X^{n+1}_{-1/2,\Delta t,h}(y^h_i)) := \mathbf{v}^{n+1}_{-1/2,\Delta t,h}(y^h_i), \tag{48}$$

  for $0 \leq n \leq N-1$. Notice that $\bigcup_{K \in \widetilde{\mathfrak{T}}^{n+1}_h} K \sim \overline{\Omega}_{t_{n+1}}$.

- **Approximate pressure in Eulerian coordinates.** In order to obtain this we use procedures analogous to the ones in the previous point. That is, we consider approximate pressure as a piecewise linear function on the moved mesh $\widetilde{\mathfrak{T}}_h^{n+1/2}$, being $\{X_{-1/2,\Delta t,h}^{n+1/2}(y_i^h)\}_{i=1}^{N_v^h}$ the vertices of this mesh. The values of the approximate pressure at vertices $\{X_{-1/2,\Delta t,h}^{n+1/2}(y_i^h)\}_{i=1}^{N_v^h}$, are obtained as follows: firstly,

$$\pi^{n+1/2}(X_{-1/2,\Delta t,h}^{n+1/2}(y_i^h)) \simeq \pi^{n+1/2}(X_{-1/2}^{n+1/2}(y_i^h)) = \pi_{-1/2}^{n+1/2}(y_i^h) \simeq \pi_{-1/2,\Delta t,h}^{n+1/2}(y_i^h),$$

and then we take

$$\pi_{\Delta t,h}^{n+1/2}(X_{-1/2,\Delta t,h}^{n+1/2}(y_i^h)) := \pi_{-1/2,\Delta t,h}^{n+1/2}(y_i^h),$$

for $0 \leq n \leq N-1$. Notice that $\bigcup_{K\in\widetilde{\mathfrak{T}}_h^{n+1/2}} K \sim \overline{\Omega}_{t_{n+1/2}}$.

Notice that for the Lagrangian schemes the computational domain is the same for all time steps. However, in order to calculate the velocity or the pressure in Eulerian coordinates, the moved mesh is used. For real fluid mechanics problems, this mesh can present large deformations. For this reason, when this happens it is necessary to remesh and reinitialize the transformation to the identity. Let us assume that we have decided to reinitialize the problem at time $t_{r-1/2}$, thus the new reference domain is $\bigcup_{K\in\widetilde{\mathfrak{T}}_h^{r-1/2}} K \sim \overline{\Omega}_{t_{r-1/2}}$.
In order to solve the problem (**LG**) in the new reference domain, we remesh this domain and calculate the new initial conditions as follows:

$$\mathbf{u}_{t_{r-1/2}}(y, t_{r-1/2}) = \mathbf{0}, \tag{49}$$

$$\mathbf{u}_{t_{r-1/2}}(y, t_{r+1/2}) = \Delta t \mathbf{v}\left(y + \mathbf{v}(y, t_r)\frac{\Delta t}{2}, t_r\right) + O(\Delta t^3) \simeq \Delta t \mathbf{v}_{\Delta t,h}^r\left(y + \mathbf{v}_{\Delta t,h}^r(y)\frac{\Delta t}{2}\right). \tag{50}$$

In order to obtain an approximate initial condition of $\mathbf{u}_{t_{r-1/2}}(y, t_{r+1/2})$ we need $\mathbf{v}_{\Delta t,h}^r$ that is calculated by using (48).
However, we want to emphasize that in the examples included in the Section 6 of the present paper, reinitialization for the pure Lagrangian method has not been used.

5.2. Semi-Lagrangian scheme

By taking $\tau = t_{n-1/2}$ and $t = t_{n+1/2}$ in (28)-(29) and using the second-order formulas (36) and (37), we obtain

$$\begin{aligned}
&\int_{\Omega_{t_{n-1/2}}} \rho^{n+1/2} \circ X_{n-1/2,\Delta t}^{n+1/2} \det F_{n-1/2,\Delta t}^{n+1/2} \frac{\mathbf{u}_{n-1/2,\Delta t}^{n+3/2} - 2\mathbf{u}_{n-1/2,\Delta t}^{n+1/2}}{\Delta t^2} \cdot \mathbf{z}\, dy - \\
&\qquad \int_{\Omega_{t_{n-1/2}}} \pi_{n-1/2,\Delta t}^{n+1/2} \det F_{n-1/2,\Delta t}^{n+1/2} (F_{n-1/2,\Delta t}^{n+1/2})^{-t} \cdot \operatorname{grad} \mathbf{z}\, dy \\
&\frac{1}{2\Delta t}\int_{\Omega_{t_{n-1/2}}} \mu^{n+1/2} \circ X_{n-1/2,\Delta t}^{n+1/2} \det F_{n-1/2,\Delta t}^{n+1/2} \operatorname{grad} \mathbf{u}_{n-1/2,\Delta t}^{n+3/2} (F_{n-1/2,\Delta t}^{n+1/2})^{-1} \\
&(F_{n-1/2,\Delta t}^{n+1/2})^{-t} \cdot \operatorname{grad} \mathbf{z}\, dy + \frac{1}{2\Delta t}\int_{\Omega_{t_{n-1/2}}} \mu^{n+1/2} \circ X_{n-1/2,\Delta t}^{n+1/2} \det F_{n-1/2,\Delta t}^{n+1/2} (F_{n-1/2,\Delta t}^{n+1/2})^{-t} \\
&(\operatorname{grad} \mathbf{u}_{n-1/2,\Delta t}^{n+3/2})^t (F_{n-1/2,\Delta t}^{n+1/2})^{-t} \cdot \operatorname{grad} \mathbf{z}\, dy = \int_{\Omega_{t_{n-1/2}}} \det F_{n-1/2,\Delta t}^{n+1/2} \mathbf{b}^{n+1/2} \circ X_{n-1/2,\Delta t}^{n+1/2} \cdot \mathbf{z}\, dy \\
&\qquad + \int_{\Gamma_{t_{n-1/2}}^N} |(F_{n-1/2,\Delta t}^{n+1/2})^{-t} \mathbf{m}_{t_{n-1/2}}| \det F_{n-1/2,\Delta t}^{n+1/2} \mathbf{h}^{n+1/2} \circ X_{n-1/2,\Delta t}^{n+1/2} \cdot \mathbf{z}\, dA_y,
\end{aligned} \tag{51}$$

$$\begin{aligned}
&\frac{1}{2\Delta t}\int_{\Omega_{t_{n-1/2}}} \det F_{n-1/2,\Delta t}^{n+1/2} \operatorname{grad} \mathbf{u}_{n-1/2,\Delta t}^{n+3/2} \cdot (F_{n-1/2,\Delta t}^{n+1/2})^{-t} q\, dy \\
&\qquad = \int_{\Omega_{t_{n-1/2}}} \det F_{n-1/2,\Delta t}^{n+1/2} g^{n+1/2} \circ X_{n-1/2,\Delta t}^{n+1/2} q\, dy,
\end{aligned} \tag{52}$$

$\forall \mathbf{z} \in \mathbf{H}^1_{\Gamma^D_{t_{n-1/2}}}(\Omega_{t_{n-1/2}})$, $\forall q \in L^2(\Omega_{t_{n-1/2}})$ and $0 \leq n \leq N-1$. In the above semi-Lagrangian problem, we have used that $\mathbf{u}^{n-1/2}_{n-1/2} \equiv \mathbf{0}$, and the following notations

$$X^{n+1/2}_{n-1/2,\Delta t}(y) = y + \mathbf{u}^{n+1/2}_{n-1/2,\Delta t}(y),$$
$$F^{n+1/2}_{n-1/2,\Delta t}(y) = I + \operatorname{grad} \mathbf{u}^{n+1/2}_{n-1/2,\Delta t}(y),$$

for $y \in \Omega_{t_{n-1/2}}$ and $0 \leq n \leq N-1$.

We propose a space discretization of the above problem by using continuous piecewise-linear+bubble finite elements for each component of the displacement and continuous piecewise-linear for pressure.

Let us suppose $\Omega_{t_{n-1/2}}$ is a bounded domain in $\mathbb{R}^d$ with a Lipschitz polygonal boundary for $0 \leq n \leq N-1$. Let us consider a suitable family of regular triangulations of $\overline{\Omega}_{t_{n-1/2}}$ to be denoted by $\mathfrak{T}^{n-1/2}_h$, consisting of elements K of diameter $\leq h$. Moreover, we assume it is compatible with the partition of the boundary into $\Gamma^D_{t_{n-1/2}}$ and $\Gamma^N_{t_{n-1/2}}$.

We consider the following spaces of finite elements:

$$X^{n-1/2}_h = \left\{ \mathbf{w}_h \in \left(C^0(\Omega_{t_{n-1/2}})\right)^d : \ \mathbf{w}_{h|_K} \in \left(P_b(K)\right)^d, \quad \forall K \in \mathfrak{T}^{n-1/2}_h \right\}, \tag{53}$$

$$X^{n-1/2}_{0h} = \left\{ \mathbf{w}_h \in X^{n-1/2}_h : \ \mathbf{w}_h = \mathbf{0} \text{ on } \Gamma^D_{t_{n-1/2}} \right\}, \tag{54}$$

$$V^{n-1/2}_h = \left\{ \varphi_h \in C^0(\Omega_{t_{n-1/2}}) : \ \varphi_{h|_K} \in P_1(K), \quad \forall K \in \mathfrak{T}^{n-1/2}_h \right\}. \tag{55}$$

In order to obtain fully discrete scheme of the time semidiscretizated problem (51)-(52) we use the approximations of function spaces $\mathbf{H}^1(\Omega_{t_{n-1/2}})$, $\mathbf{H}^1_{\Gamma^D_{t_{n-1/2}}}(\Omega_{t_{n-1/2}})$ and $L^2(\Omega_{t_{n-1/2}})$ given by (53), (54) and (55), respectively. Moreover, by using procedures analogous to the ones in the previous section we obtain the approximate initial and boundary conditions for the displacement.
Thus, we obtain the following fully discrete problem:

$(\mathbf{SLG})_2$.– Find two sequence of functions $\{\mathbf{u}^{n+3/2}_{n-1/2,\Delta t,h}\}_{n=0}^{N-1} \in \prod_{n=0}^{N-1} X^{n-1/2}_h$ and $\{\pi^{n+1/2}_{n-1/2,\Delta t,h}\}_{n=0}^{N-1} \in \prod_{n=0}^{N-1} V^{n-1/2}_h$ such that

$$\begin{aligned}
&\int_{\Omega_{t_{n-1/2}}} \rho^{n+1/2} \circ X^{n+1/2}_{n-1/2,\Delta t,h} \det F^{n+1/2}_{n-1/2,\Delta t,h} \frac{\mathbf{u}^{n+3/2}_{n-1/2,\Delta t,h} - 2\mathbf{u}^{n+1/2}_{n-1/2,\Delta t,h}}{\Delta t^2} \cdot \mathbf{z}_h \, dy - \\
&\qquad \int_{\Omega_{t_{n-1/2}}} \pi^{n+1/2}_{n-1/2,\Delta t,h} \det F^{n+1/2}_{n-1/2,\Delta t,h} (F^{n+1/2}_{n-1/2,\Delta t,h})^{-t} \cdot \operatorname{grad} \mathbf{z}_h \, dy \\
&\qquad \frac{1}{2\Delta t} \int_{\Omega_{t_{n-1/2}}} \mu^{n+1/2} \circ X^{n+1/2}_{n-1/2,\Delta t,h} \det F^{n+1/2}_{n-1/2,\Delta t,h} \operatorname{grad} \mathbf{u}^{n+3/2}_{n-1/2,\Delta t,h} \\
&\qquad\qquad (F^{n+1/2}_{n-1/2,\Delta t,h})^{-1} (F^{n+1/2}_{n-1/2,\Delta t,h})^{-t} \cdot \operatorname{grad} \mathbf{z}_h \, dy \\
&+ \frac{1}{2\Delta t} \int_{\Omega_{t_{n-1/2}}} \mu^{n+1/2} \circ X^{n+1/2}_{n-1/2,\Delta t,h} \det F^{n+1/2}_{n-1/2,\Delta t,h} (F^{n+1/2}_{n-1/2,\Delta t,h})^{-t} (\operatorname{grad} \mathbf{u}^{n+3/2}_{n-1/2,\Delta t,h})^t \\
&\quad (F^{n+1/2}_{n-1/2,\Delta t,h})^{-t} \cdot \operatorname{grad} \mathbf{z}_h \, dy = \int_{\Omega_{t_{n-1/2}}} \det F^{n+1/2}_{n-1/2,\Delta t,h} \mathbf{b}^{n+1/2} \circ X^{n+1/2}_{n-1/2,\Delta t,h} \cdot \mathbf{z}_h \, dy \\
&\quad + \int_{\Gamma^N_{t_{n-1/2}}} |(F^{n+1/2}_{n-1/2,\Delta t,h})^{-t} \mathbf{m}_{t_{n-1/2}}| \det F^{n+1/2}_{n-1/2,\Delta t,h} \mathbf{h}^{n+1/2} \circ X^{n+1/2}_{n-1/2,\Delta t,h} \cdot \mathbf{z}_h \, dA_y, \\
&\qquad\qquad \forall \mathbf{z}_h \in X^{n-1/2}_{0h},
\end{aligned} \tag{56}$$

$$\begin{aligned}&\frac{1}{2\Delta t}\int_{\Omega_{t_{n-1/2}}} \det F^{n+1/2}_{n-1/2,\Delta t,h}\,\mathrm{grad}\,\mathbf{u}^{n+3/2}_{n-1/2,\Delta t,h}\cdot(F^{n+1/2}_{n-1/2,\Delta t,h})^{-t}q_h\,dy\\ &=\int_{\Omega_{t_{n-1/2}}}\det F^{n+1/2}_{n-1/2,\Delta t,h}g^{n+1/2}\circ X^{n+1/2}_{n-1/2,\Delta t,h}q_h\,dy,\ \forall q_h\in V_h^{n-1/2},\end{aligned}\tag{57}$$

with

$$\mathbf{u}^{n+1/2}_{n-1/2,\Delta t,h}(y)=\Delta t\mathbf{v}^n_{\Delta t,h}\left(y+\mathbf{v}^n_{\Delta t,h}(y)\frac{\Delta t}{2}\right),\ \text{for all node } y \text{ of mesh } \mathfrak{T}_h^{n-1/2},\tag{58}$$

$$\mathbf{u}^{n+3/2}_{n-1/2,\Delta t,h}(y)=\mathbf{u}^{n+1/2}_{n-1/2,\Delta t,h}(y)+\Delta t\mathbf{v}_D^{n+1}\left(y+\mathbf{v}_D^{n-1/2}(y)\frac{3}{2}\Delta t\right)\ \text{for all node } y \text{ on } \Gamma^D_{t_{n-1/2}},\tag{59}$$

for $0\le n\le N-1$, where $\mathbf{v}^n_{\Delta t,h}$ is an approximation of the spatial velocity calculated as explained below and

$$X^{n+1/2}_{n-1/2,\Delta t,h}(y)=y+\mathbf{u}^{n+1/2}_{n-1/2,\Delta t,h}(y),\quad F^{n+1/2}_{n-1/2,\Delta t,h|K}=I+\mathrm{grad}\,\mathbf{u}^{n+1/2}_{n-1/2,\Delta t,h|K},$$

for $y\in\Omega_{t_{n-1/2}}$, $K\in\mathfrak{T}_h^{n-1/2}$ and $0\le n\le N-1$. Notice that this problem is analogous to the one in the previous section but reinitializing the transformation to the identity at each time step.

By using procedures analogous to the ones in the previous section, we can obtain approximations of the pressure in Eulerian coordinates, the velocity and the motion, by using the solution of problem $(\mathbf{SLG})_2$.

- **Approximate velocity relative to $\Omega_{t_{n-1/2}}$ at time t_{n+1}: $\mathbf{v}^{n+1}_{n-1/2,\Delta t,h}$.** It can be easily obtained by using (17) and a second-order centered formula to approximate $\dfrac{\partial\mathbf{u}_\tau}{\partial t}$. More precisely, since

$$\begin{aligned}\mathbf{v}^{n+1}_{n-1/2}(y)=\frac{\partial\mathbf{u}_{n-1/2}}{\partial t}(y,t_{n+1})&=\frac{\mathbf{u}^{n+3/2}_{n-1/2}(y)-\mathbf{u}^{n+1/2}_{n-1/2}(y)}{\Delta t}+O(\Delta t^2)\\ &\simeq\frac{\mathbf{u}^{n+3/2}_{n-1/2,\Delta t,h}(y)-\mathbf{u}^{n+1/2}_{n-1/2,\Delta t,h}(y)}{\Delta t},\end{aligned}$$

  we take

$$\mathbf{v}^{n+1}_{n-1/2,\Delta t,h}(y):=\frac{\mathbf{u}^{n+3/2}_{n-1/2,\Delta t,h}(y)-\mathbf{u}^{n+1/2}_{n-1/2,\Delta t,h}(y)}{\Delta t},$$

  for $y\in\Omega_{t_{n-1/2}}$ and $0\le n\le N-1$.

- **Approximate motion relative to $\Omega_{t_{n-1/2}}$ at time t_{n+1}: $X^{n+1}_{n-1/2,\Delta t,h}$.** Noting that $\mathbf{u}_\tau(y,t)=X_\tau(y,t)-y$ and using a second-order centred formula, we obtain

$$X^{n+1}_{n-1/2}(y)=y+\frac{\mathbf{u}^{n+3/2}_{n-1/2}(y)+\mathbf{u}^{n+1/2}_{n-1/2}(y)}{2}+O(\Delta t^2).$$

  Then we define the approximation

$$X^{n+1}_{n-1/2,\Delta t,h}(y):=y+\frac{\mathbf{u}^{n+3/2}_{n-1/2,\Delta t,h}(y)+\mathbf{u}^{n+1/2}_{n-1/2,\Delta t,h}(y)}{2},$$

  for $y\in\Omega_{t_{n-1/2}}$ and $0\le n\le N-1$.

- **Approximate velocity in Eulerian coordinates at time t_{n+1}: $\mathbf{v}^{n+1}_{\Delta t,h}$.** Let us denote by $\{y_i^h\}_{i=1}^{N_v^h}$ the vertices of mesh $\mathfrak{T}_h^{n-1/2}$. Notice that these vertices can depend on time instant. For simplicity, we do not explicit this dependence. In order to obtain an approximate velocity in Eulerian coordinates, we consider this is piecewise linear on the moved mesh $\widetilde{\mathfrak{T}}_h^{n+1}$, being $\{X^{n+1}_{n-1/2,\Delta t,h}(y_i^h)\}_{i=1}^{N_v^h}$

the vertices of this mesh. The values of the approximate velocity at vertices $\{X^{n+1}_{n-1/2,\Delta t,h}(y^h_i)\}_{i=1}^{N^h_v}$, can be obtained by using $\mathbf{v}^{n+1}_{n-1/2,\Delta t,h}$. Since we have

$$\mathbf{v}^{n+1}(X^{n+1}_{n-1/2,\Delta t,h}(y^h_i)) \simeq \mathbf{v}^{n+1}(X^{n+1}_{n-1/2}(y^h_i)) = \mathbf{v}^{n+1}_{n-1/2}(y^h_i) \simeq \mathbf{v}^{n+1}_{n-1/2,\Delta t,h}(y^h_i),$$

we take the approximation

$$\mathbf{v}^{n+1}_{\Delta t,h}(X^{n+1}_{n-1/2,\Delta t,h}(y^h_i)) := \mathbf{v}^{n+1}_{n-1/2,\Delta t,h}(y^h_i),$$

for $0 \leq n \leq N-1$. Notice that $\bigcup_{K\in\widetilde{\mathfrak{T}}^{n+1}_h} K \sim \overline{\Omega}_{t_{n+1}}$.

- **Approximate pressure in Eulerian coordinates at time $t_{n+1/2}$: $\pi^{n+1/2}_{\Delta t,h}$.** In order to obtain the pressure values in Eulerian coordinates, we consider the approximate pressure as a piecewise linear function on the moved mesh $\widetilde{\mathfrak{T}}^{n+1/2}_h$, being $\{X^{n+1/2}_{n-1/2,\Delta t,h}(y^h_i)\}_{i=1}^{N^h_v}$ the vertices of this mesh. The values of the approximate pressure at vertices $\{X^{n+1/2}_{n-1/2,\Delta t,h}(y^h_i)\}_{i=1}^{N^h_v}$, are obtained as follows: firstly,

$$\pi^{n+1/2}(X^{n+1/2}_{n-1/2,\Delta t,h}(y^h_i)) \simeq \pi^{n+1/2}(X^{n+1/2}_{n-1/2}(y^h_i)) = \pi^{n+1/2}_{n-1/2}(y^h_i) \simeq \pi^{n+1/2}_{n-1/2,\Delta t,h}(y^h_i),$$

and then we take

$$\pi^{n+1/2}_{\Delta t,h}(X^{n+1/2}_{n-1/2,\Delta t,h}(y^h_i)) := \pi^{n+1/2}_{n-1/2,\Delta t,h}(y^h_i),$$

for $0 \leq n \leq N-1$. Notice that $\bigcup_{K\in\widetilde{\mathfrak{T}}^{n+1/2}_h} K \sim \overline{\Omega}_{t_{n+1/2}}$.

We also recall that, when we are calculating $\mathbf{u}^{n+3/2}_{n-1/2,\Delta t,h}$, $\mathbf{v}^n_{\Delta t,h}$ is known.

For the semi-Lagrangian schemes the computational domain changes at each time step. In general, $\Omega_{t_{n-1/2}}$ is unknown; instead we calculate an approximation by using the approximate motion.

Remark 5.3. *If we approximate $X^{n+1/2}_{n-1/2,\Delta t,h}(y)$ by y and $F^{n+1/2}_{n-1/2,\Delta t,h}(y)$ by I in problem $(\mathbf{SLG})_2$, then a new semi-Lagrangian problem is obtained. Notice that these approximations are of first order in time. This first order semi-Lagrangian method will be denoted by $(\mathbf{SLG})_1$. If $\Omega_t = \Omega$ for all t and the coefficients ρ and η are time independent, then the matrix associated with this method is independent of time.*

6. Numerical results

In order to assess the performance of the above numerical methods, analyze their rates of convergence and compare them, we solve three test problems in two space dimensions. The first one is an academic problem, for which we verify rates of convergence for the pure Lagrangian and the semi-Lagrangian methods described in the present paper. The second one is the lid driven cavity problem. It models the flow in a square box driven by the motion of the lid of the box. This problem has been solved with the semi-Lagrangian methods presented in this paper and the obtained numerical results are compared with a reference solution. Finally, the third example is a free surface problem. More precisely, we consider a classical example of sloshing numerical simulation. This problem has been solved with the pure Lagrangian method proposed in this paper.

In Example 1, we calculate the error between discrete solutions $\mathbf{v}_{\Delta t,h}$ and $\pi_{\Delta t,h}$, and exact solutions $\mathbf{v}$ and π. For this, we approximate the theoretical $L^2(\Omega_{t_{n+1}})$ and $L^2(\Omega_{t_{n-1/2}})$ norms by using a quadrature formula exact for polynomials of degree 2. Moreover, domains $\Omega_{t_{n+1}}$ and $\Omega_{t_{n-1/2}}$ are calculated by using the approximate motion. The function spaces endowed with these norms are denoted by $L^2_h(\Omega_{t_{n+1}})$ and $L^2_h(\Omega_{t_{n-1/2}})$, respectively. Thus, we denote by $l^\infty(\mathcal{A}^n)$, being $\mathcal{A}^n = L^2_h(\Omega_{t_{n+1}}), L^2_h(\Omega_{t_{n-1/2}})$, the space of sequences in $\{\mathcal{A}^n\}_{n=0}^{N-1}$ equipped with the norm $\left|\left|\widehat{\Psi}\right|\right|_{l^\infty(\mathcal{A}^n)} := \max_{n=0}^{N-1} ||\Psi^n||_{\mathcal{A}^n}$.
Moreover, schemes $(\mathbf{LG})$, $(\mathbf{SLG})_2$ and $(\mathbf{SLG})_1$ were combined with an exact quadrature formula for polynomials of degree 5 in all of the terms.

Example 1
This is a problem aiming to check the rates of convergence of the schemes proposed in this paper.

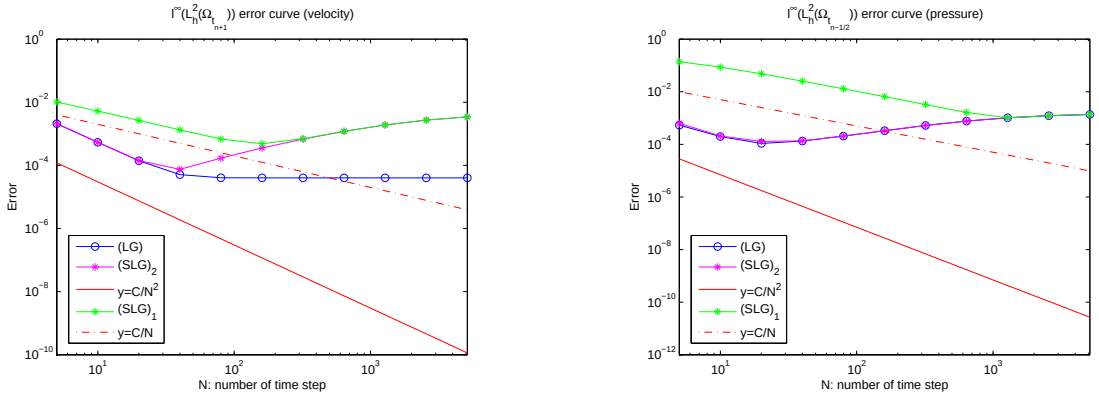

Figure 2: Example 1: computed $l^\infty(L_h^2(\Omega_{t_{n+1}}))$ velocity error (left) and $l^\infty(L_h^2(\Omega_{t_{n-1/2}}))$ pressure error (right) versus the number of time steps in log-log scale, for a fixed spatial mesh of 125×125 vertices.

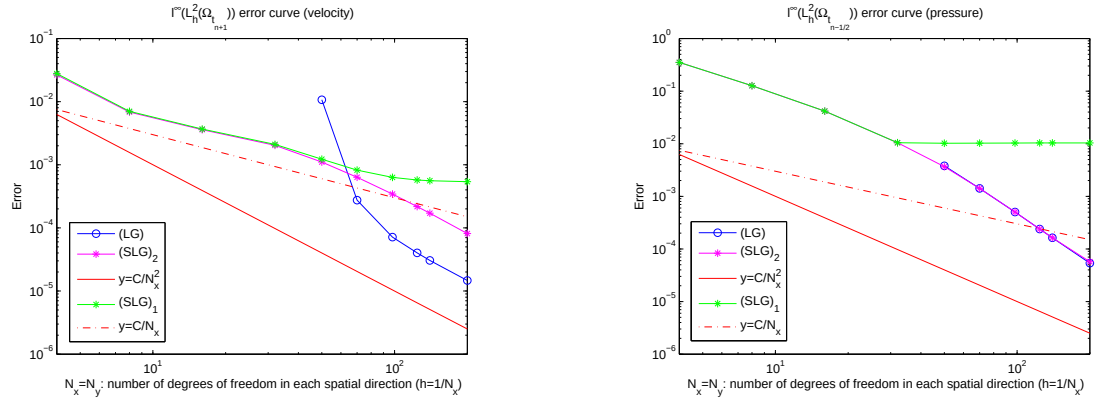

Figure 3: Example 1: computed $l^\infty(L_h^2(\Omega_{t_{n+1}}))$ velocity error (left) and $l^\infty(L_h^2(\Omega_{t_{n-1/2}}))$ pressure error (right) versus $1/h$ in log-log scale, for $\Delta t = 0.01$.

The spatial domain is $\Omega = (0,1) \times (0,1)$, $t_0 = 0$ and $T = 1$. The diffusion tensor is $A = 0.001I$ and $\rho = 1$. Functions $\mathbf{b}$ and g and Dirichlet boundary and initial conditions are taken such that the exact solution is

$$\begin{aligned} \pi(x,y) &= 10(2x-1)(2y-1), \\ v_1(x,y,t) &= 10te^t x^2(x-1)^2 y(y-1)(2y-1), \\ v_2(x,y,t) &= -10te^t x(x-1)(2x-1)y^2(y-1)^2. \end{aligned}$$

We solve this problem by using methods $(\mathbf{LG})$, $(\mathbf{SLG})_2$ and $(\mathbf{SLG})_1$. In Figure 2, we have fixed a uniform spatial mesh of 125×125 vertices and shown the $l^\infty\left(L_h^2(\Omega_{t_{n+1}})\right)$ velocity error (left) and $l^\infty\left(L_h^2(\Omega_{t_{n-1/2}})\right)$ pressure error (right) versus the number of time steps. These results show that schemes $(\mathbf{LG})$ and $(\mathbf{SLG})_2$ possess second-order accuracy in time and scheme $(\mathbf{SLG})_1$ possess first-order accuracy in time. Concerning the semi-Lagrangian schemes, for fixed h, we can observe an increasing error as the time step decreases below a threshold. This is due to the presence of terms added by the quadrature formula to the error. In Figure 3 we represent the $l^\infty\left(L_h^2(\Omega_{t_{n+1}})\right)$ velocity error and the $l^\infty\left(L_h^2(\Omega_{t_{n-1/2}})\right)$ pressure error versus $1/h$ for a fixed small time step, namely $\Delta t = 0.01$. We can observe that schemes $(\mathbf{LG})$, $(\mathbf{SLG})_2$ possess second-order accuracy in space in the $l^\infty(L^2)$-norm. Moreover, with the scheme $(\mathbf{SLG})_1$ we observe first-order accuracy in space for velocity and second-order accuracy in space for pressure.

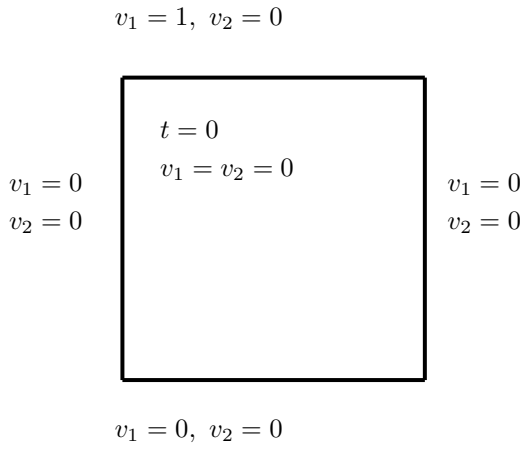

Figure 4: Driven cavity: initial and boundary conditions.

Remark 6.1. *In the academic tests, we have observed that the order of the error of the methods is maintained if we calculate F without considering the bubble term. In some cases, in order to not to have negative values of* $\det F$ *it is convenient to do this.*

Example 2
We consider a driven cavity flow governed by the incompressible Navier-Stokes equations to compare the numerical results obtained with the classical semi-Lagrangian methods and the new ones presented in this paper. The driven cavity problem has long been used as a test case for Navier-Stokes solvers, thanks to it has simple geometry and boundary conditions. Although the problem looks simple in many ways, the flow in a cavity retains all the flow physics with counter rotating vortices appearing at the corners of the cavity. In some papers in the literature, a steady solution is sought and therefore the numerical solution of steady incompressible Navier-Stokes equations are presented at various Reynolds numbers (see, for instance, [21], [15], [16], [6]). However, in other papers the bifurcation of the flow in a driven cavity from a steady regime to an unsteady regime is studied (see, for instance, [18], [20]). The dimensionless problem is defined in a square domain $\Omega = (0,1) \times (0,1)$ with the upper side of the cavity sliding to the right at unit velocity. The problem is depicted in Figure 4. For the current study, the problem was solved for a Reynolds number of 1000 on a series of meshes, the coarsest mesh having 17×17 vertices, while the finest one has 70962 vertices. We solve this problem with semi-Lagrangian methods $(\mathbf{SLG})_1$ and $(\mathbf{SLG})_2$ and with the second-order in time semi-Lagrangian classical method given by (34)-(35) combined with continuous piecewise-linear+bubble finite elements for each component of the velocity and continuous piecewise-linear for pressure for space discretization. This method will be denoted by $(\mathbf{SLG})_2^2$; we use the strategy given in [3] to calculate the integrals. We carry the simulations along the time until convergence. Results are compared with the benchmark solutions given in [21].

In Figure 5 we have fixed the time step, namely, $\Delta t = 0.002$ and show, for different regular meshes, the horizontal velocity profiles along the vertical centreline of the cavity (on the left) and the vertical velocity profiles along the horizontal centreline of the cavity (on the right), computed by using the $(\mathbf{SLG})_2$, $(\mathbf{SLG})_1$ and $(\mathbf{SLG})_2^2$ methods. The benchmark solutions of Ghia is included for comparison. Clearly, $(\mathbf{SLG})_2$ and $(\mathbf{SLG})_1$ achieve better results than the corresponding classical second-order method $(\mathbf{SLG})_2^2$. Moreover, under the same parameters, the $(\mathbf{SLG})_2$ and $(\mathbf{SLG})_1$ schemes provide the same numerical solutions. Besides, for both methods, errors with Δt in the denominator are observed (see Figures 5 and 6). However, for this example, the matrix associated with the $(\mathbf{SLG})_1$ scheme is time independent. Moreover, in order to obtain a stationary numerical solution, with the $(\mathbf{SLG})_2$ scheme we need to use smaller time steps than with the $(\mathbf{SLG})_1$ method. For these reasons, in this case, the most convenient method to solve this problem is the $(\mathbf{SLG})_1$ scheme. In Figure 6 we have shown, for different regular meshes, the horizontal velocity profiles along the vertical centreline of the cavity (on the left)

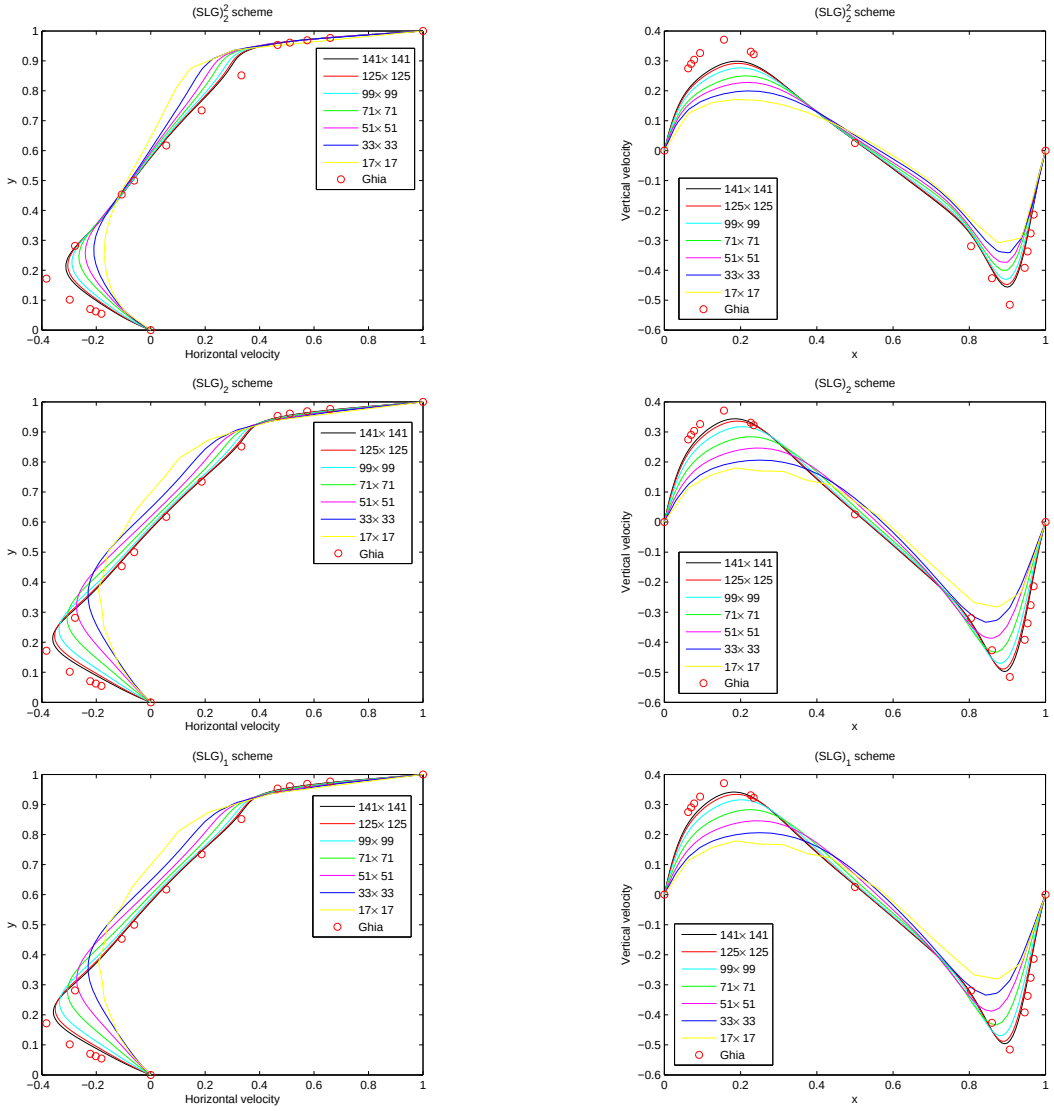

Figure 5: Driven cavity: on the left, profiles of the horizontal velocity along the vertical centreline, calculated using different schemes for a range of mesh sizes, and compared with the benchmark solutions given in [21]. On the right, profiles of the vertical velocity along the horizontal centreline, calculated using different schemes for a range of mesh sizes, and compared with the benchmark solutions given in [21].

and the vertical velocity profiles along the horizontal centreline of the cavity (on the right), computed by using the $(\mathbf{SLG})_1$ method. In this figure, the time step varies with the mesh. More precisely, for each mesh, we consider the largest time step for which the orientation of the elements of the moved mesh $\widetilde{\mathfrak{T}}_h^{n+1}$ is the same as the one of the elements of the mesh $\mathfrak{T}_h^{n-1/2}$. In Figure 7 we represent the numerical solution obtained with the $(\mathbf{SLG})_1$ method for a spatial mesh of 70962 vertices and $\Delta t = 0.0026$. More precisely, the horizontal velocity profiles along the vertical centreline of the cavity, the vertical velocity profiles along the horizontal centreline of the cavity and the isovelocity and streamfunction contours are plotted. As the references in the literature, our numerical solutions exhibits a large primary vortex with two secondary vortices in the two bottom corners.

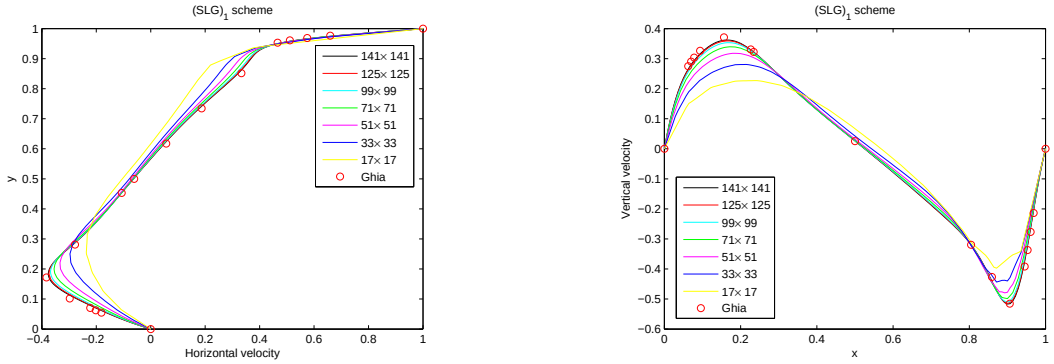

Figure 6: Driven cavity: on the left, profiles of the horizontal velocity along the vertical centreline, calculated using the $(\mathbf{SLG})_1$ scheme for a range of mesh sizes, and compared with the benchmark solutions given in [21]. On the right, profiles of the vertical velocity along the horizontal centreline, calculated using the $(\mathbf{SLG})_1$ scheme for a range of mesh sizes, and compared with the benchmark solutions given in [21]. For each mesh, we use the largest possible time step.

Example 3

To show the behaviour of the pure Lagrangian formulation for large mesh distortion, the analysis of large amplitude sloshing in a rectangular tank has been carried out. The width of the tank is $0.8\,m$ and the depth is $0.3\,m$. Incompressible fluid is considered. The liquid in the tank is subject to a sinusoidal horizontal acceleration. More precisely, the body force is

$$\mathbf{b}(x,t) = \rho(x,t)(A \cdot g \cdot sin(\omega t), -g),$$

where A is an arbitrary constant governing the amplitude of the excitation, g is the gravity acceleration and ω is the excitation frequency. In this example, $A = 0.01$, $\rho = 1000\,kg/m^3$, $g = 9.8\,m/s^2$ and $\omega = 5.642\,rad/s$. Using these parameters, experimental results show that the resonance frequency of the tank is $0.898Hz$. At the vertical boundaries the horizontal velocity is zero, at the lower horizontal boundary the vertical velocity is zero and at the upper horizontal boundary we impose null Neumann condition (force-free). Since it is a free surface problem we solve it with the pure Lagrangian method (**LG**) without reinitializing. Notice that in pure Lagrangian methods the computational domain is the reference domain; in this case it is $\Omega = (0, 0.8) \times (0, 0.3)$. We solve this problem for different viscosity values, $\mu = 0.1, 0.01, 0.001$. Figure (8) shows the vertical displacement of the upper corner nodes at the wall tank, as a function of time. The results are in good agreement with those given in [23] and [28]. In Figure 9 we represent an instantaneous configuration of the domain and the streamlines.

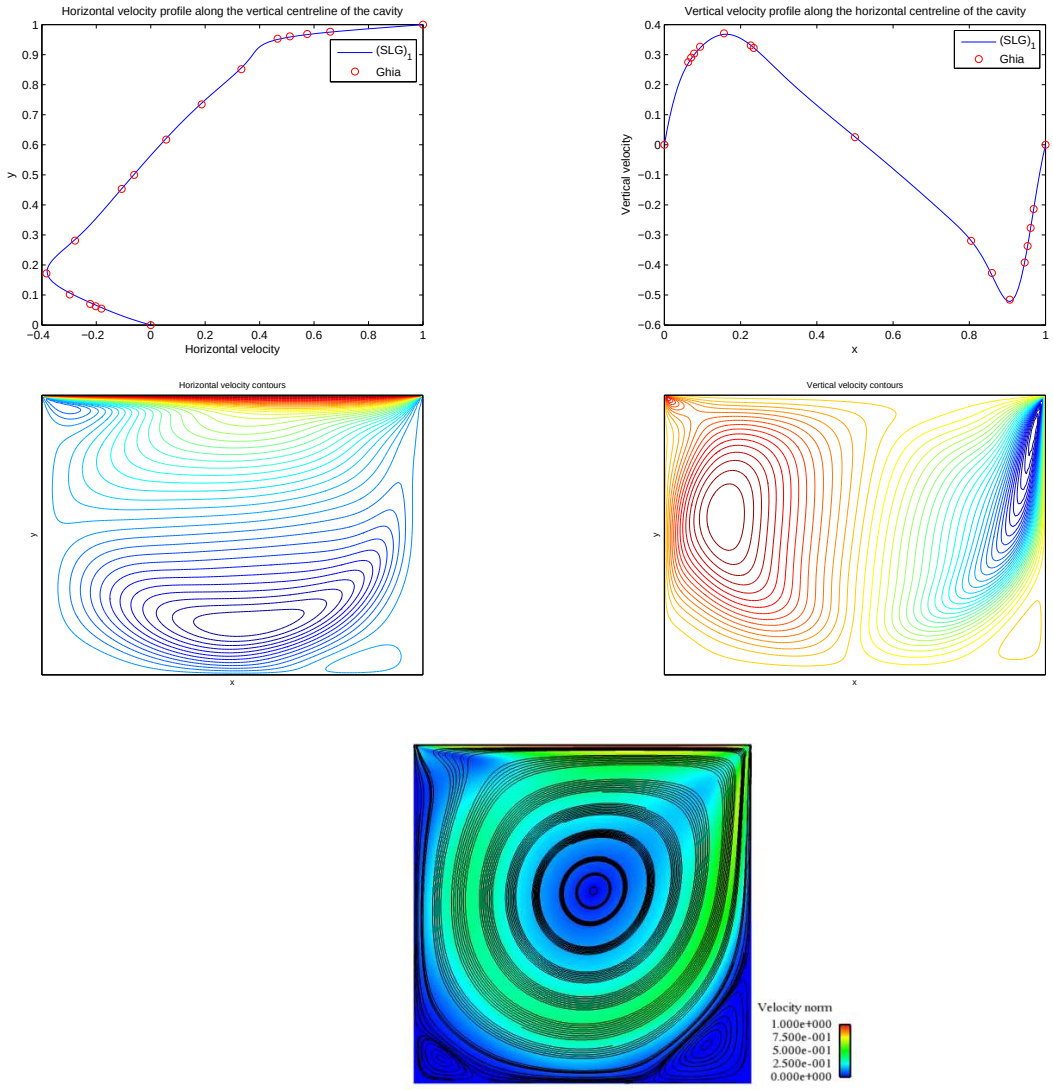

Figure 7: Driven cavity: horizontal velocity profiles along the vertical centreline of the cavity, the vertical velocity profiles along the horizontal centreline of the cavity and the isovelocity and streamfunction (bottom) contours, computed with the $(\mathbf{SLG})_1$ method, for a spatial mesh of 70962 vertices and $\Delta t = 0.0026$.

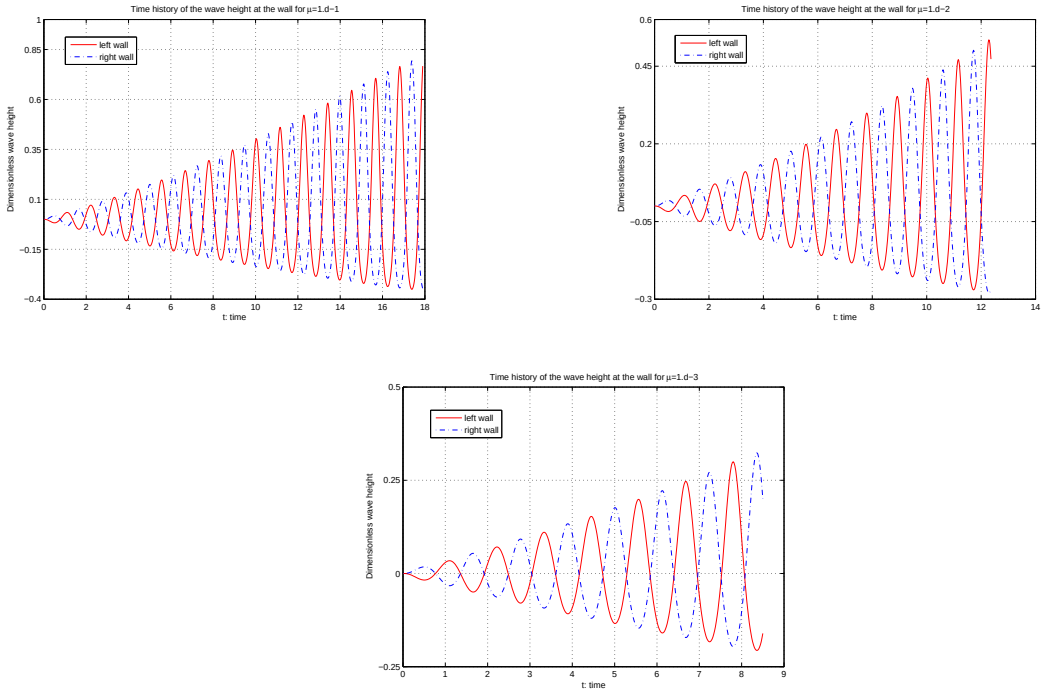

Figure 8: Sloshing waves: time history of wave height at the walls for $\mu = 0.1$ (top left), $\mu = 0.01$ (top right) and $\mu = 0.001$ (bottom), and for a spatial mesh of 5743 vertices and $\Delta t = 0.02$.

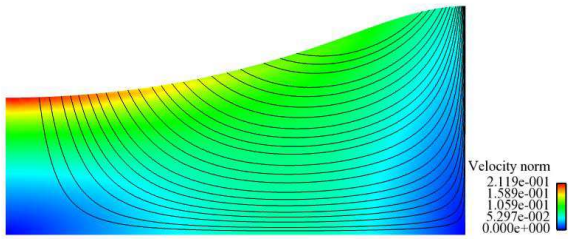

Figure 9: Sloshing waves: instantaneous domain configuration and streamlines for $\mu = 0.001$ at $t = 8.35$, and for a spatial mesh of 5743 vertices and $\Delta t = 0.02$.

7. Conclusions

We have obtained a unified formulation with which classical and new characteristics methods can be obtained for solving the Navier-Stokes equations. In particular, we have proposed two new Lagrange-Galerkin schemes in terms of the displacement, one pure Lagrangian and another one semi-Lagrangian. The semi-Lagrangian scheme is analogous to the pure Lagrangian method but reinitializing the transformation to the identity at each time step. Numerical tests have been presented to compare the new and classical methods, assess the performance of the new numerical methods and analyze their rates of convergence. We have observed that the new schemes achieve better results than the classical ones. Moreover, we have considered a free surface problem. It has been solved with the pure Lagrangian displacement method proposed in this paper. These new characteristics methods are useful for solving free surface problems because the computational domain is time independent. However, when the mesh elements have high distortions it is necessary to remesh and reinitialize the transformation to the identity. In fact, for solving some problems with high Reynolds numbers, it is convenient to use semi-Lagrangian schemes.

References

[1] M. Bause, P. Knabner, Uniform error analysis for Lagrange-Galerkin approximations of convection-dominated problems, SIAM. J. Numer. Anal. 39 (2002) 1954–1984.

[2] M. Benítez, A. Bermúdez, Pure Lagrangian and semi-Lagrangian finite element methods for the numerical solution of convection-diffusion problems (to apppear in Int. J. Numer. Anal. Mod.).

[3] M. Benítez, A. Bermúdez, A second order characteristics finite element scheme for natural convection problems, J. Comput. Appl. Math. 235 (2011) 3270–3284.

[4] M. Benítez, A. Bermúdez, Numerical Analysis of a second-order pure Lagrange-Galerkin method for convection-diffusion problems. Part I: time discretization, SIAM. J. Numer. Anal. 50 (2012) 858–882.

[5] M. Benítez, A. Bermúdez, Numerical Analysis of a second-order pure Lagrange-Galerkin method for convection-diffusion problems. Part II: fully discretized scheme and numerical results, SIAM. J. Numer. Anal. 50 (2012) 2824–2844.

[6] A.S. Benjamin, V.E. Denny, On the convergence of numerical solutions for 2-d flows in a cavity at large Re, J. Comput. Phys. 33 (1979) 340–358.

[7] A. Bermúdez, J. Durany, La méthode des caracteristiques pour des problèmes de convection-diffusion stationnaires, M2AN. Math. Mod. and Num. Anal. 21 (1987) 7–26.

[8] A. Bermúdez, M.R. Nogueiras, C. Vázquez, Numerical analysis of convection-diffusion-reaction problems with higher order characteristics/finite elements. Part I: Time discretization, SIAM. J. Numer. Anal. 44 (2006) 1829–1853.

[9] A. Bermúdez, M.R. Nogueiras, C. Vázquez, Numerical analysis of convection-diffusion-reaction problems with higher order characteristics/finite elements. Part II: Fully discretized scheme and quadrature formulas, SIAM. J. Numer. Anal. 44 (2006) 1854–1876.

[10] K. Boukir, Y. Maday, B. Métivet, E. Razafindrakoto, A high-order characteristics/finite element method for the incompressible Navier-Stokes equations, Internat. J. Numer. Methods Fluids 25 (1997) 1421–1454.

[11] K. Chrysafinos, N.J. Walkington, Error estimates for discontinuous Galerkin approximations of implicit parabolic equations, SIAM J. Numer. Anal. 43 (2006) 2478–2499.

[12] K. Chrysafinos, N.J. Walkington, Error estimates for the discontinuous Galerkin methods for parabolic equations, SIAM J. Numer. Anal. 44 (2006) 349–366.

[13] K. Chrysafinos, N.J. Walkington, Lagrangian and moving mesh methods for the convection diffusion equation, M2AN Math. Model. Numer. Anal. 42 (2008) 25–55.

[14] J. Douglas, Jr., T.F. Russell, Numerical methods for convection-dominated diffusion problems based on combining the method of characteristics with finite element or finite difference procedures, SIAM J. Numer. Anal. 19 (1982) 871–885.

[15] E. Erturk, T.C. Corke, C. Gokcol, Numerical solutions of 2-D steady incompressible driven cavity flow at high Reynolds numbers, Int. J. Numer. Methods Fluids 48 (2005) 747–774.

[16] E. Erturk, C. Gokcol, Fourth order compact formulation of Navier-Stokes equations and driven cavity flow at high Reynolds numbers, Int. J. Numer. Methods Fluids 50 (2006) 421–736.

[17] R.E. Ewing, H. Wang, A summary of numerical methods for time-dependent advection-dominated partial differential equations, J. Comput. Appl. Math. 128 (2001) 423–445.

[18] A. Fortin, M. Jardak, J.J. Gervais, R. Pierre, Localization of Hopf bifurcations in fluid flow problems, Int. J. Numer. Methods Fluids 24 (1997) 1185–1210.

[19] G. Fourestey, Stabilité des méthodes de Lagrange-Galerkin du premier et du second ordre, tech. report, INRIA, RR 4505 (2002). http://hal.inria.fr/inria-00072083.

[20] J.J. Gervais, D. Lemelin, , R. Pierre, Some experiments with stability analysis of discrete incompressible flows in the lid-driven cavity, Int. J. Numer. Methods Fluids 24 (1997) 477–492.

[21] U. Ghia, K.N. Ghia, C.T. Shin, High-Re solutions for incompressible flow using the Navier-Stokes equations and a multigrid method, J. Comput. Phys. 48 (1982) 387–411.

[22] M.E. Gurtin, An Introduction to Continuum Mechanics, volume 158, Academic Press, San Diego, 1981.

[23] A. Huerta, W.K. Liu, Viscous flow with large free surface motion, Comput. Methods Appl. Mech. Engrg. 69 (1988) 277–324.

[24] K.W. Morton, A. Priestley, E. Süli, Stability of the Lagrange-Galerkin method with non-exact integration, M2AN Math. Model. Numer. Anal. 22 (1998) 625–653.

[25] O. Pironneau, On the transport-diffusion algorithm and its applications to the Navier-Stokes equations, Numer. Math. 38 (1982) 309–332.

[26] A. Priestley, Exact projections and the Lagrange-Galerkin method: a realistic alternative to quadrature, J. Comput. Phys. 112 (1994) 316–333.

[27] H. Rui, M. Tabata, A second order characteristic finite element scheme for convection-diffusion problems, Numer. Math. 92 (2002) 161–177.

[28] M. Souli, J.P. Zolesio, Arbitrary Lagrangian-Eulerian and free surface methods in fluid mechanics, Comput. Methods Appl. Mech. Engrg. 191 (2001) 451–466.

[29] E. Süli, Stability and convergence of the Lagrange-Galerkin method with non-exact integration. Academic Press, London, The mathematics of finite elements and applications, VI (1988) 435–442.

[30] M. Tabata, S. Fujima, Robustness of a characteristic finite element scheme of second order in time increment, Computational Fluid Dynamics 2004 (2006) 177–182.